Effect of oxygen isotope substitution on magnetic ordering in $(La_{1-y}Pr_y)_{0.7}Ca_{0.3}MnO_3$

V. Pomjakushin
Laboratory for Neutron Scattering, ETH Zürich and PSI, Villigen

A. Balagurov
I.M. Frank Laboratory of Neutron Physics, JINR, Dubna

D. Sheptyakov
Laboratory for Neutron Scattering, ETH Zurich and PSI, Villigen

K. Conder, E. Pomjakushina
Laboratory for Developments and Methods, PSI
Laboratory for Neutron Scattering, ETH Zürich and PSI, Villigen

Large isotope effect in metallic manganites

Decrease in ($T_C \sim t^*$) by $^{16}O \rightarrow {}^{18}O$ exchange

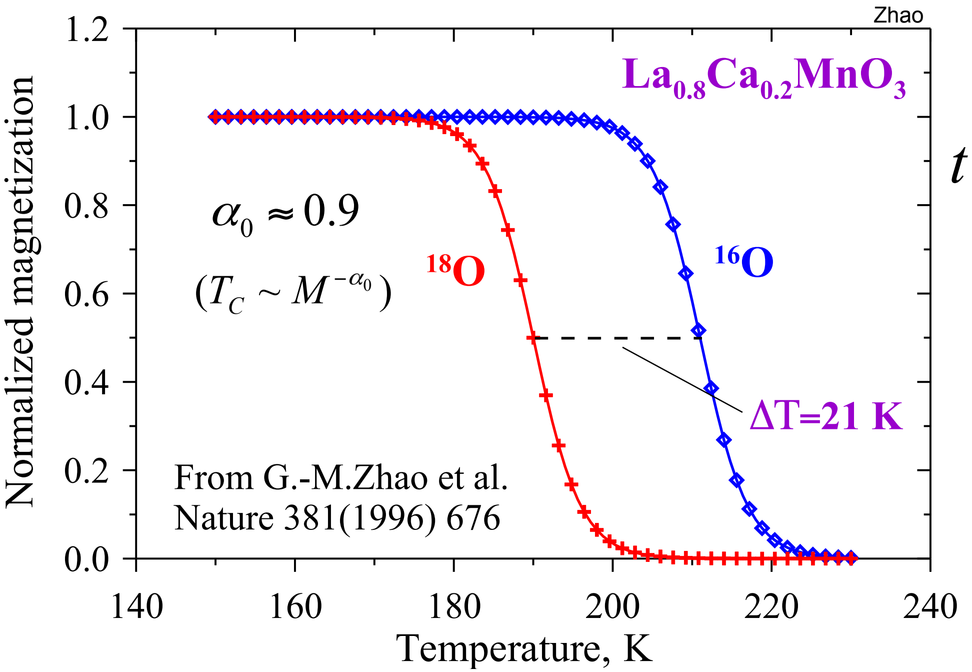

Polaronic narrowing[1-3] of bandwidth t

$$t^* = t\exp(-g^2)$$,where $g^2 = \lambda \cdot t/\omega$

coupl. const

$$\omega \sim M^{-0.5}$$

$$\alpha_0 = -\Delta \ln T_C / \Delta \ln M \sim 0.5E/\hbar\omega$$

Oxygen isotope exponent $(T_C \sim M^{-\alpha_0})$

$$\alpha_0 = -\Delta \ln T_C / \Delta \ln M$$

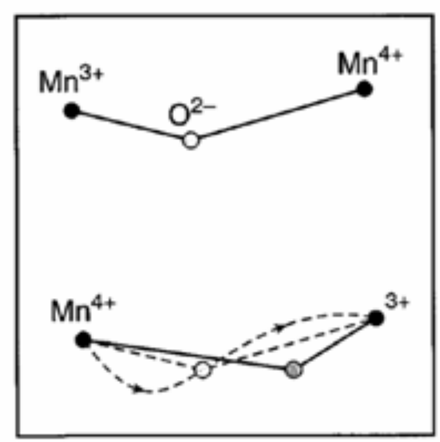

Schematic of possible dynamic distortion

$\alpha_0 \approx 0.8 - 1$ can be theoretically estimated[1]

[1] L. P. Gor' kov and V. Z. Kresin, Phys. Rep. **400**, 149 (2004).
[2] A.S.Alexandrov, N.F.Mott Int. J. Mod. Phys **8,** 2075 (1994)
[3] A.S.Alexandrov, V.V.Kabanov, D.K.Ray, PRB **49,** 9915 (1994)

Isotope effect expected if:

Polaronic narrowing works:

e-hopping time $\tau \sim 1/\omega$ opt. phonon ~20 meV

Isotope effect expected?

YES	NO
double-exchange charge ordering $T_C \sim zt^*$ $T_{CO} \sim t^*/V$, $V \sim 0.2$	Superexchange $J_{AF} \sim -b^2/U$ $J_F \sim b^3/U^2$ $\tau = \hbar/U$, $U \sim 5$eV

<u>Isotope effect allows us to verify the type of interactions involved!</u>

Giant isotope effect in intermediate-bandwidth manganites

$^{16}O \longrightarrow {}^{18}O$

$T_C \longrightarrow 0$ K?

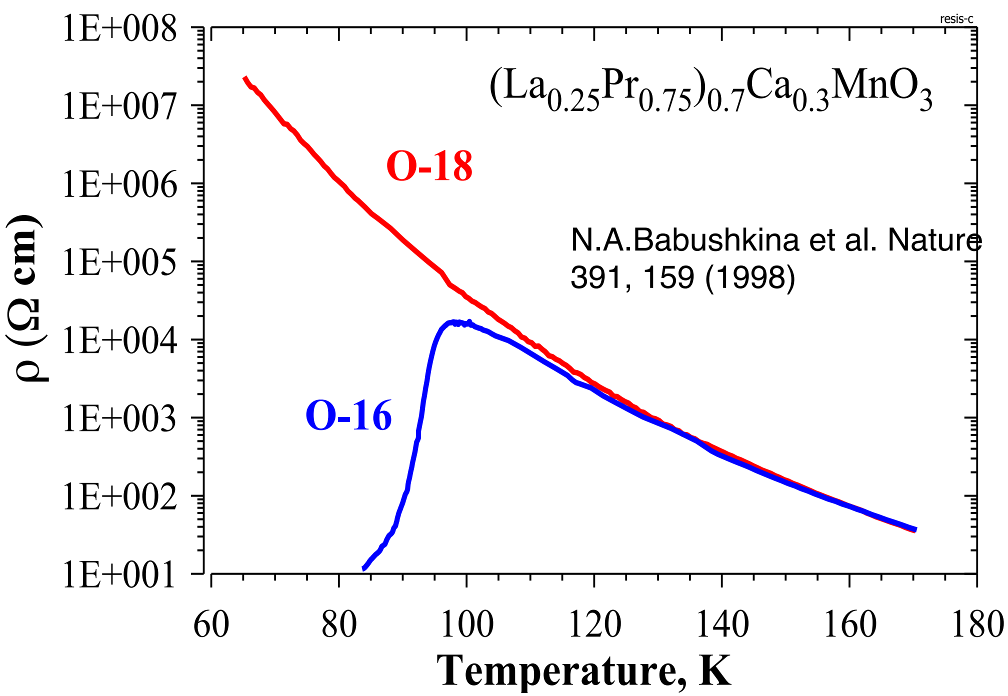

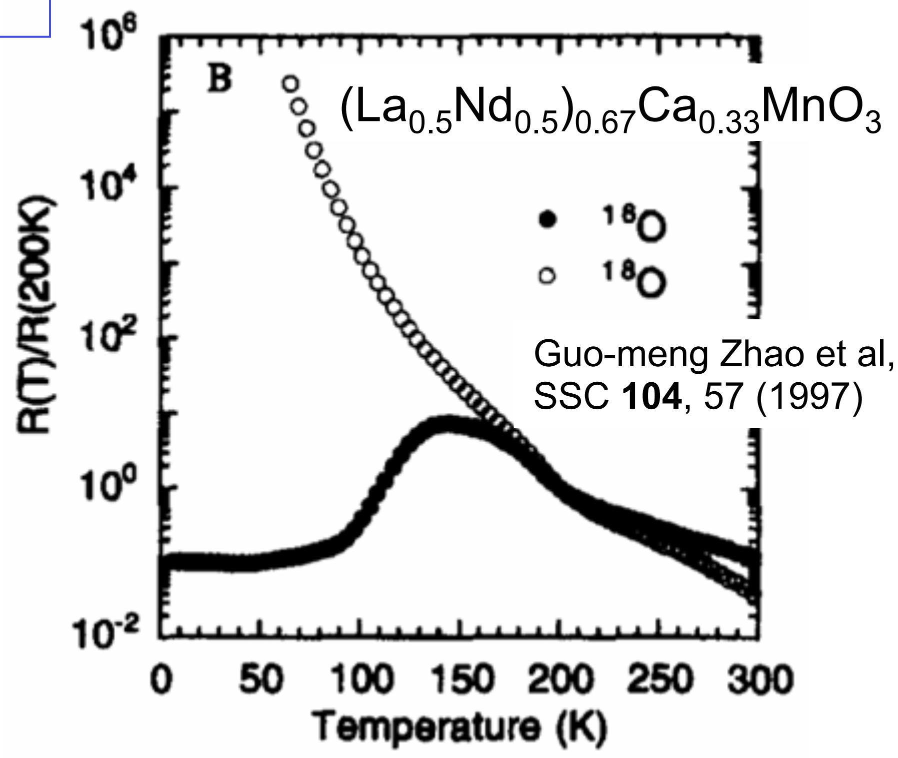

$$t^* = t\exp(-\frac{E_{pol}}{\varpi})$$ is not enough!

$(La_{1-y}Pr_y)_{0.7}Ca_{0.3}MnO_3$ phase diagram

A-cation

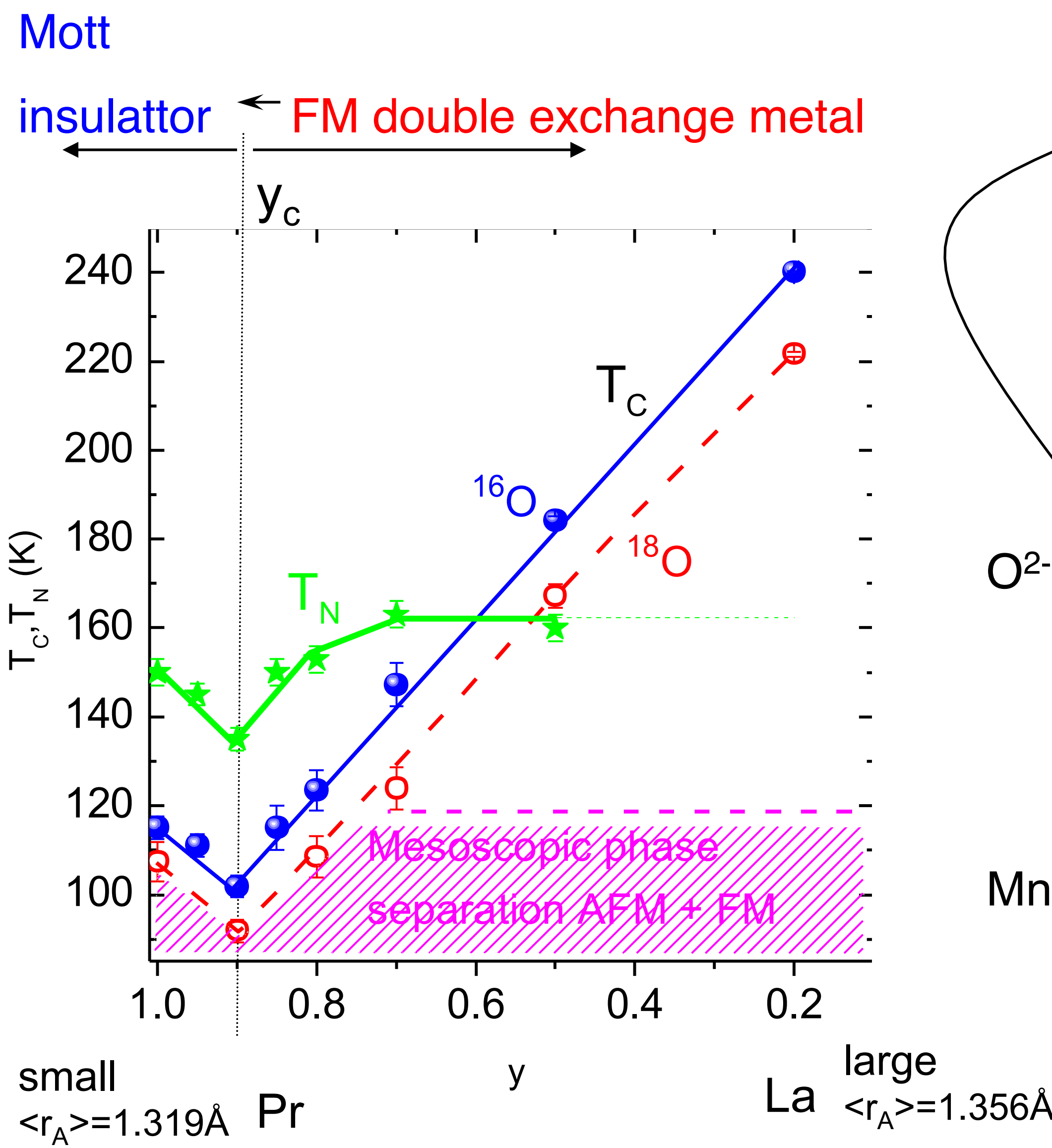

(Mn-O) electron transfer integral
$b_\sigma \sim \cos(\phi) \sim <r_A> \sim (1\text{-}const\cdot y)$
is increased with *y* resulting in the insulator-metal transition

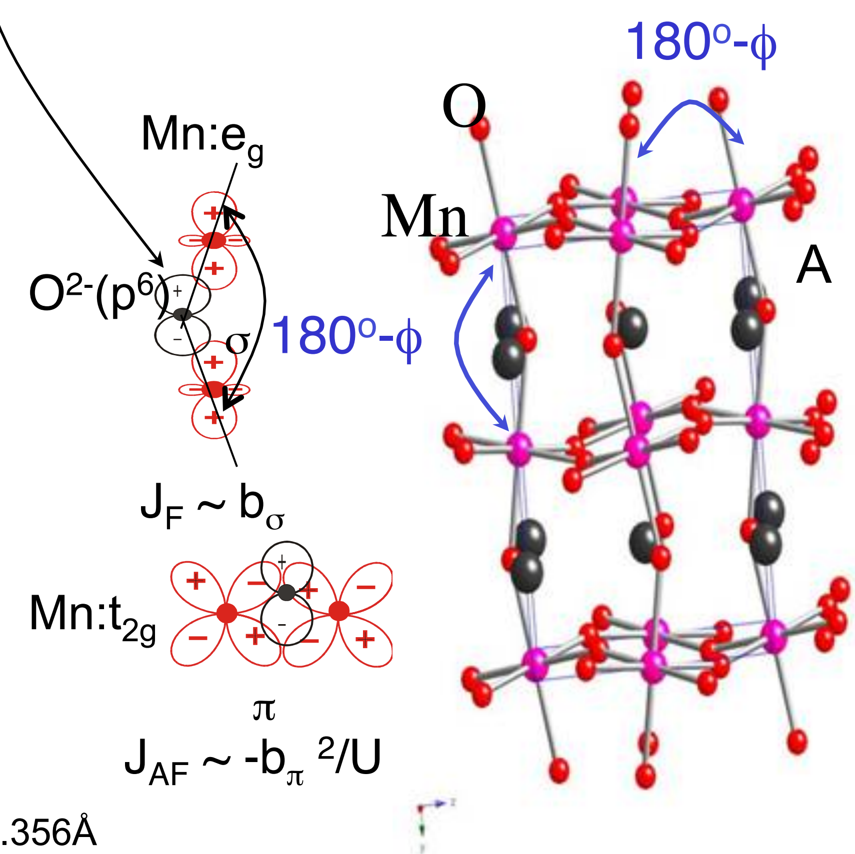

$(La_{1-y}Pr_y)_{0.7}Ca_{0.3}MnO_3$ phase diagram

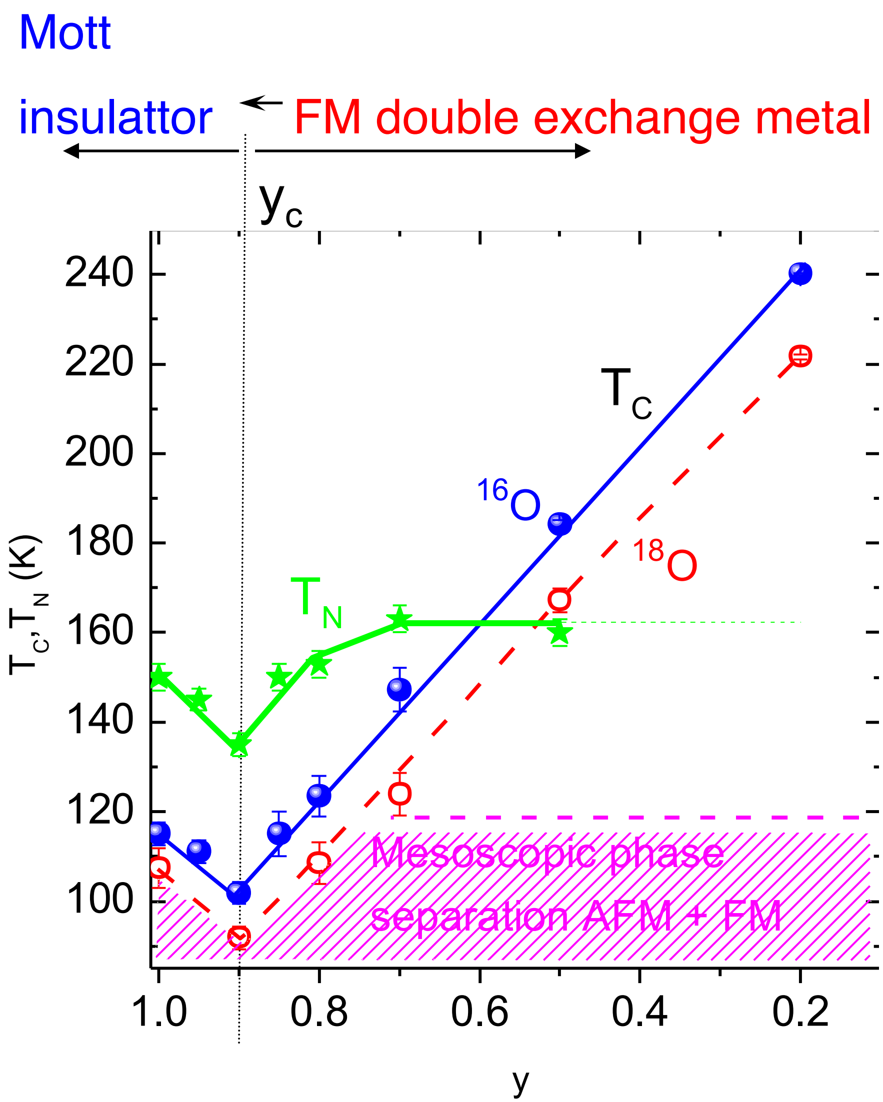

$T_C \sim \phi$

Mn-O-Mn valence bond angles

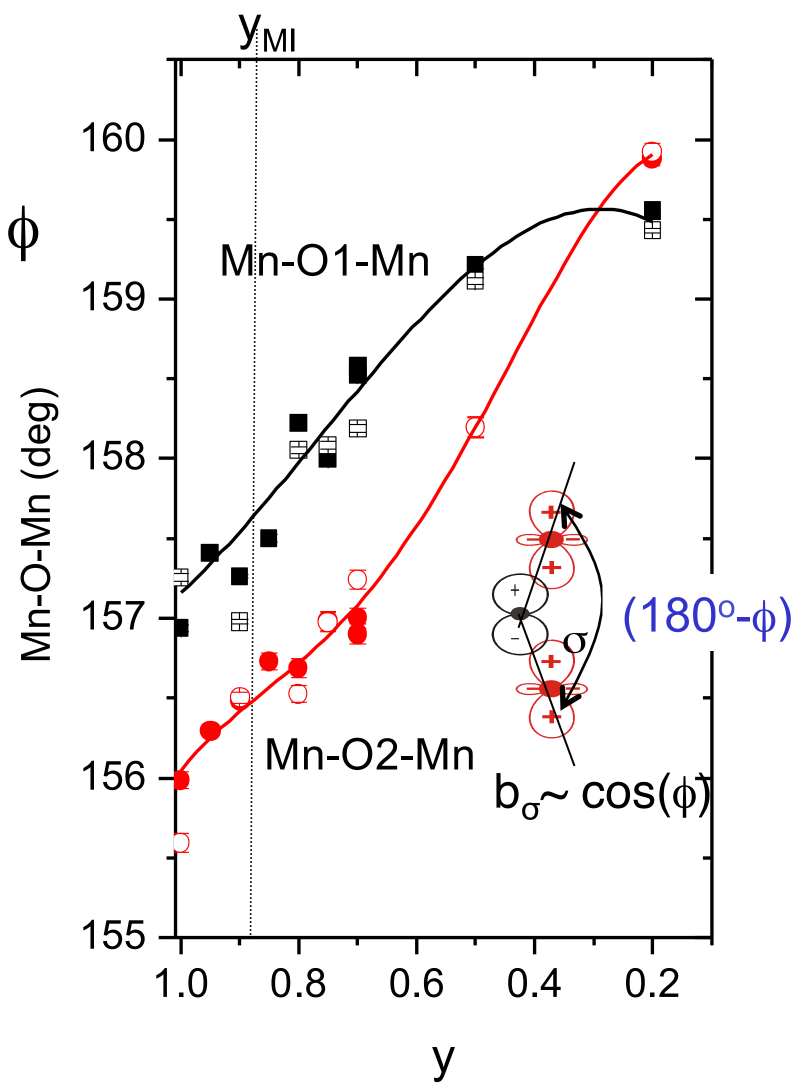

Questions

- How the Orbital (OO), charge (CO) and magnetic ordering (AFM, FM) depend on temperature and the effective bandwidth (Pr conc. y, oxygen mass)?
- What is the ground magnetic state? Factors controlling phase separation.
- Origin of the giant isotope effect?
- Microscopic mechanism of phase separation.

Experiment

1. Neutron (T=2-1400K) and synchrotron x-ray (room T) diffraction

High resolution HRPT diffractometer,
Cold DMC (up to 4.2Å) at SINQ/PSI

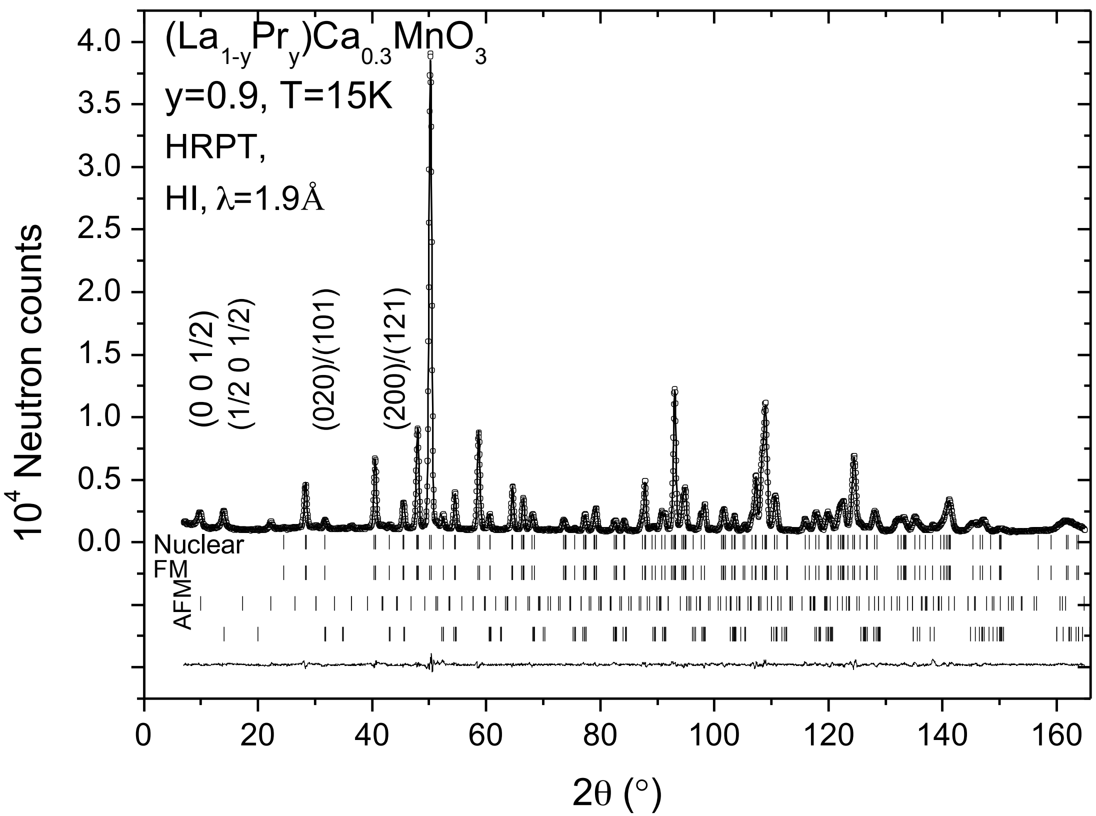

MS beamline at SLS/PSI

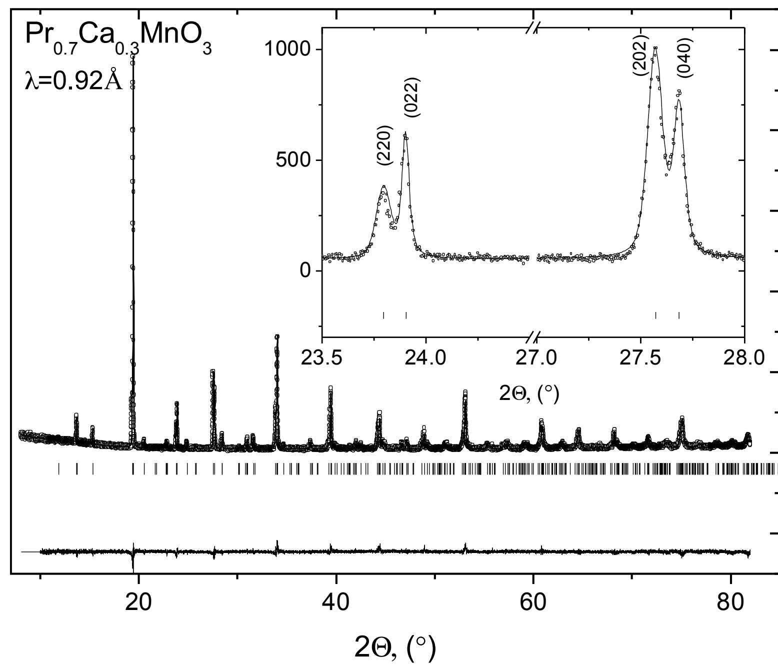

2. ac-magnetic susceptibility, T=2K-400K, DSC

Crystal structure: pseudocubic-orthorhombic transition

$(La_{1-y}Pr_y)_{0.7}Ca_{0.3}MnO_3$

A-cation

The micro-strains is an intrinsic property of this system due to:

1. A-cation radius dispersion

2. structure transformation

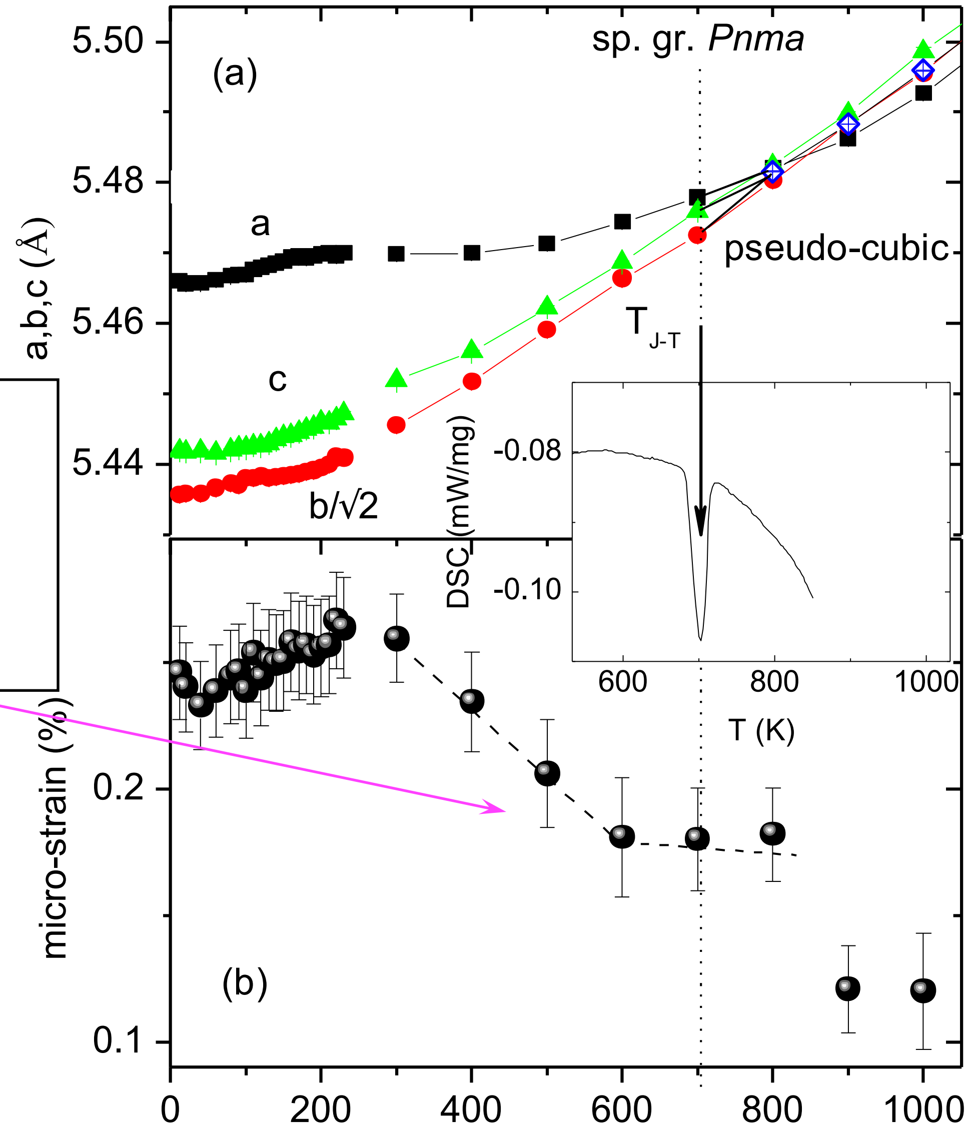

Orbital and charge ordering OO/CO (I)

$(La_{1-y}Pr_y)_{0.7}Ca_{0.3}(Mn^{3+})_{0.7}(Mn^{4+})_{0.3}O_3$ $Mn^{3+} : Mn^{4+}$ = (70:30)%

(Mn^{3+}): $3t_{2g}1e_g$ (Mn^{4+}): $3t_{2g}$

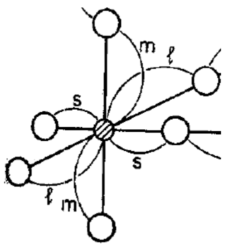

$$|\theta\rangle = \cos\frac{\theta}{2}|3z^2-r^2\rangle + \sin\frac{\theta}{2}|x^2-y^2\rangle$$

$$\mathrm{tg}(\theta) = \frac{Q_2}{Q_3} = \frac{\sqrt{3}(l-s)}{(2m-l-s)}$$

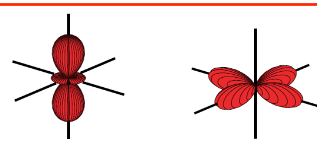

pseudo-spin plane

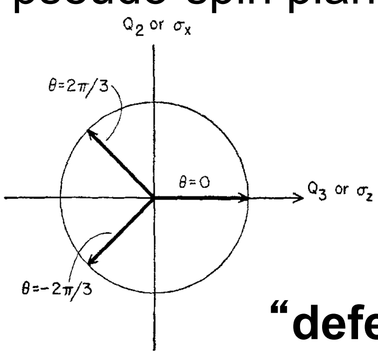

"defect" CO model:

$$Mn^{4+}(\%) = \frac{1}{2} - \frac{m-s}{l-s} \cong 26\%$$

Mn-O bond lengths in LPCM (y=0.7)

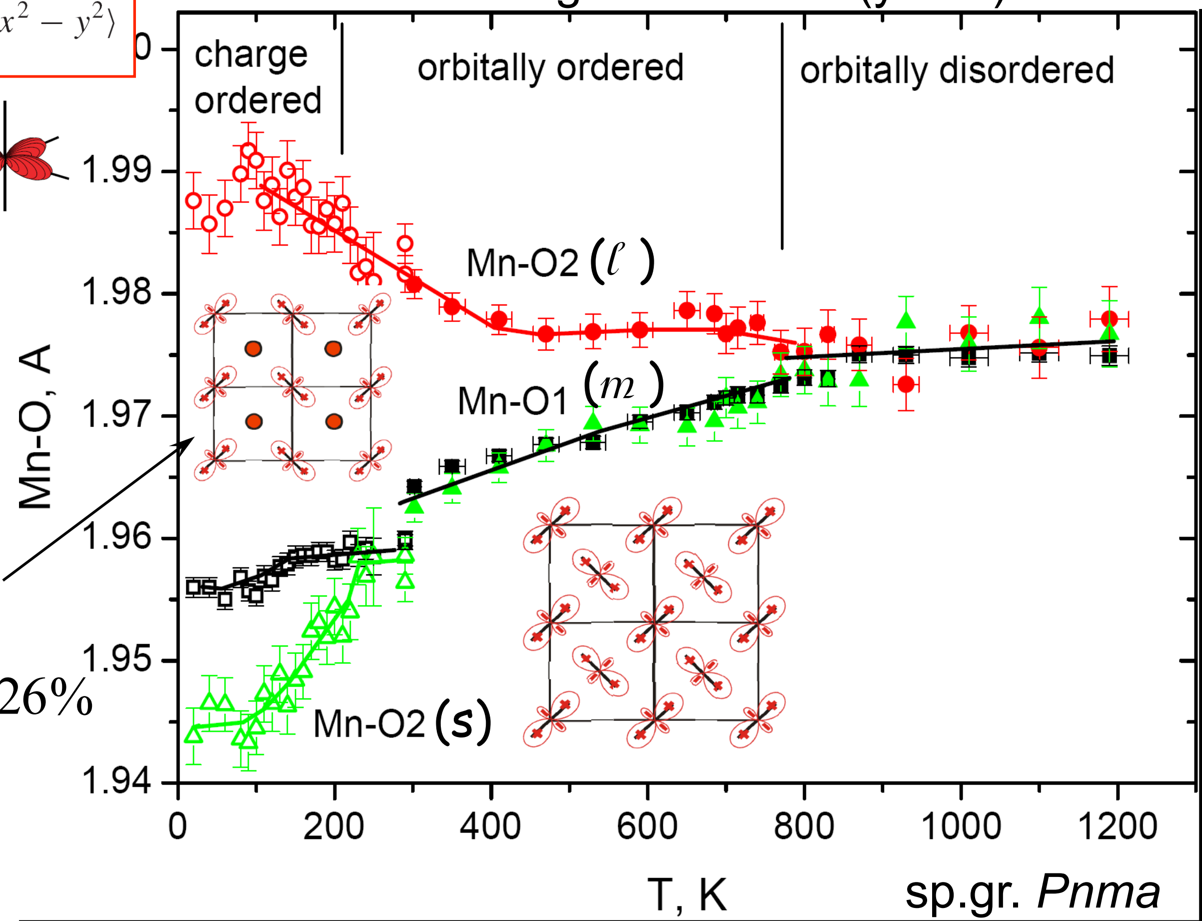

Orbital and charge ordering OO/CO (II)

$(La_{1-y}Pr_y)_{0.7}Ca_{0.3}(Mn^{3+})_{0.7}(Mn^{4+})_{0.3}O_3$

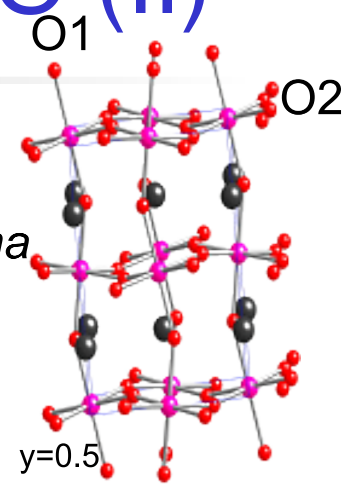

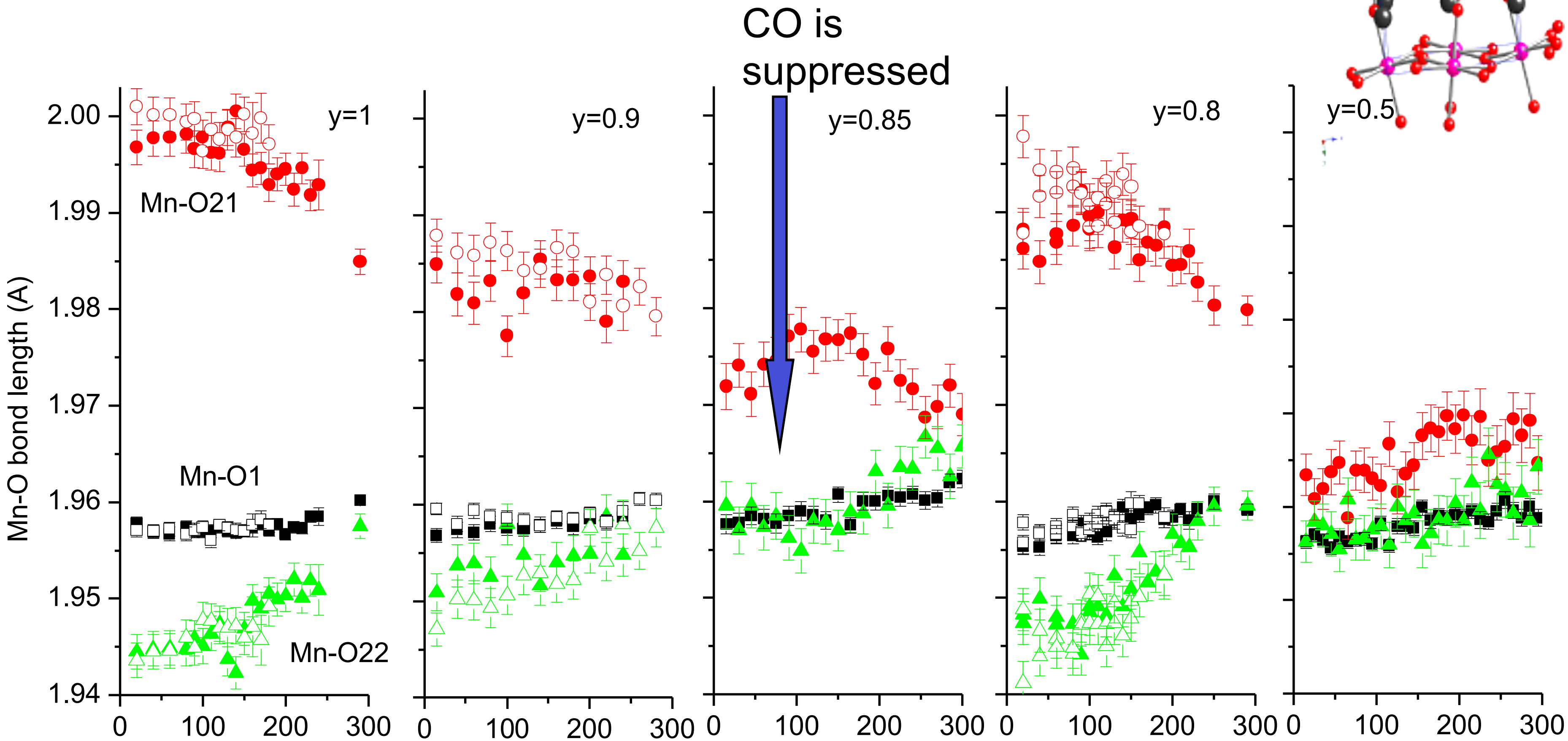

Microstructure parameters

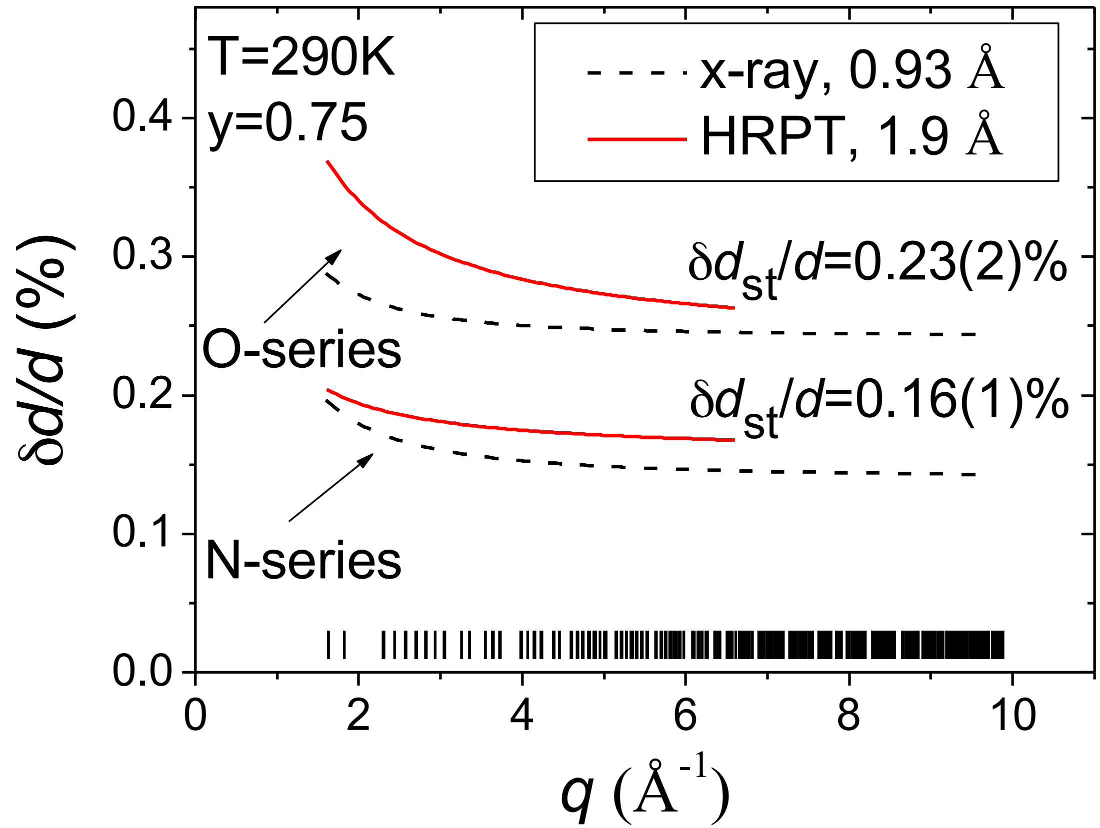

Bragg peak width

$\delta d/d = \delta a/a \otimes d/L \otimes$ "instrument"

strain size

De-convolution of the pseudo-Voigt Bragg peaks width $\delta(2\theta)$="*Cagliotti*" with the instrument resolution function.

Anisotropic micro-strain - structure indicator of CO

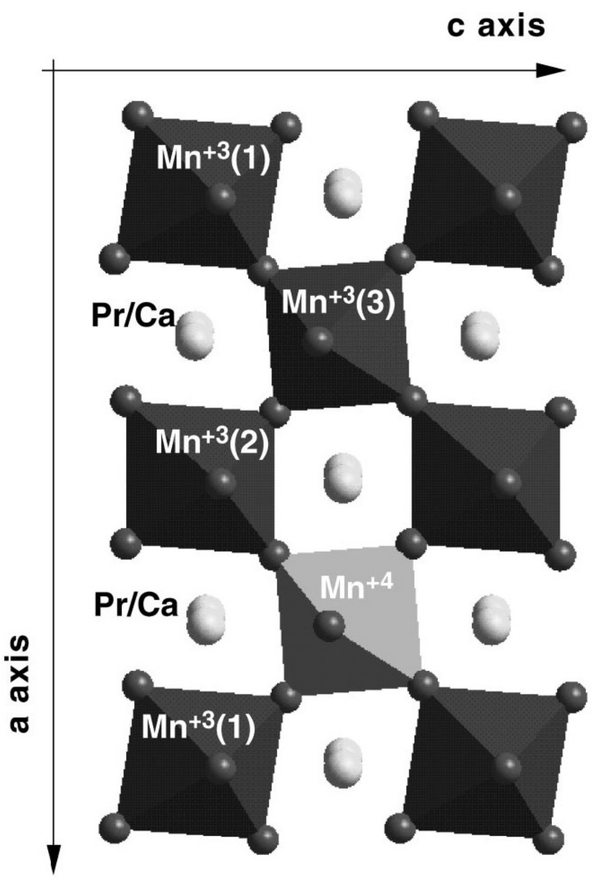

Picture rom D.E. Cox et al.,PRB (1998)

Anisotropic micro-strain along [100]

~ a measure of CO

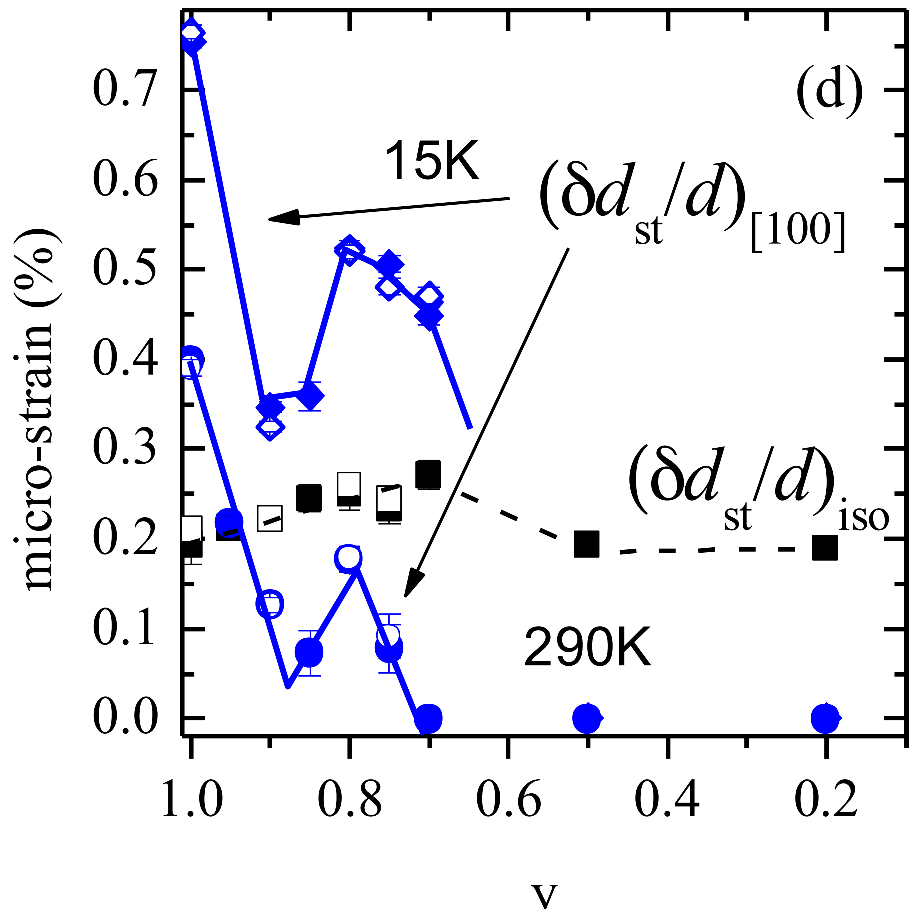

micro-strains as a function of Pr concentration (sp. gr. *Pnma*)

Magnetic ordering as a function of temperature

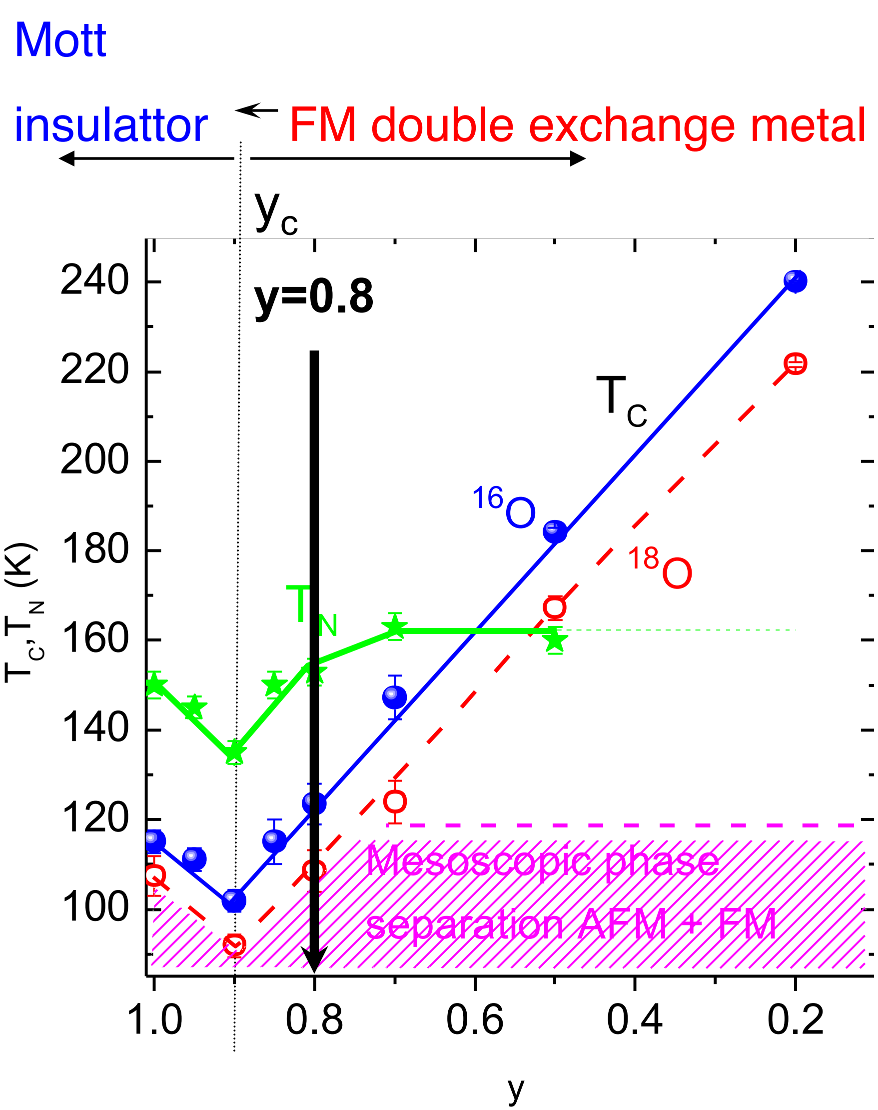

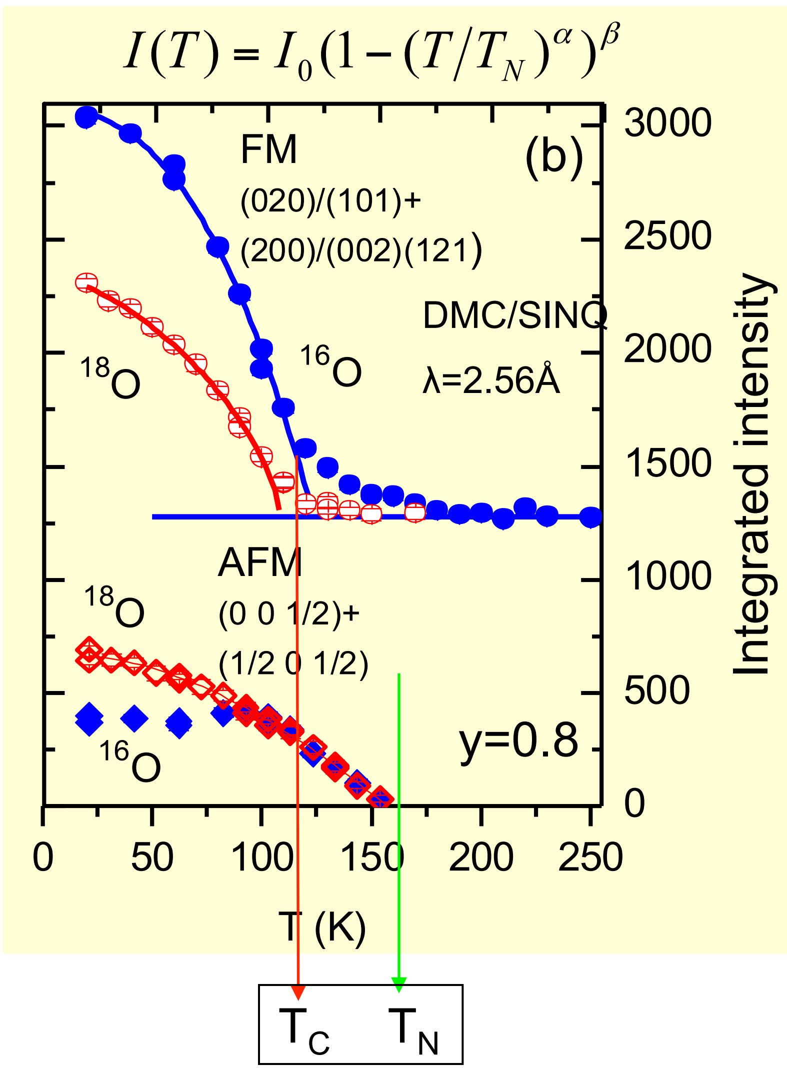

Magnetic ground state of $(La_{1-y}Pr_y)_{0.7}Ca_{0.3}MnO_3$

Effective FM moment as a function of Pr-conc.

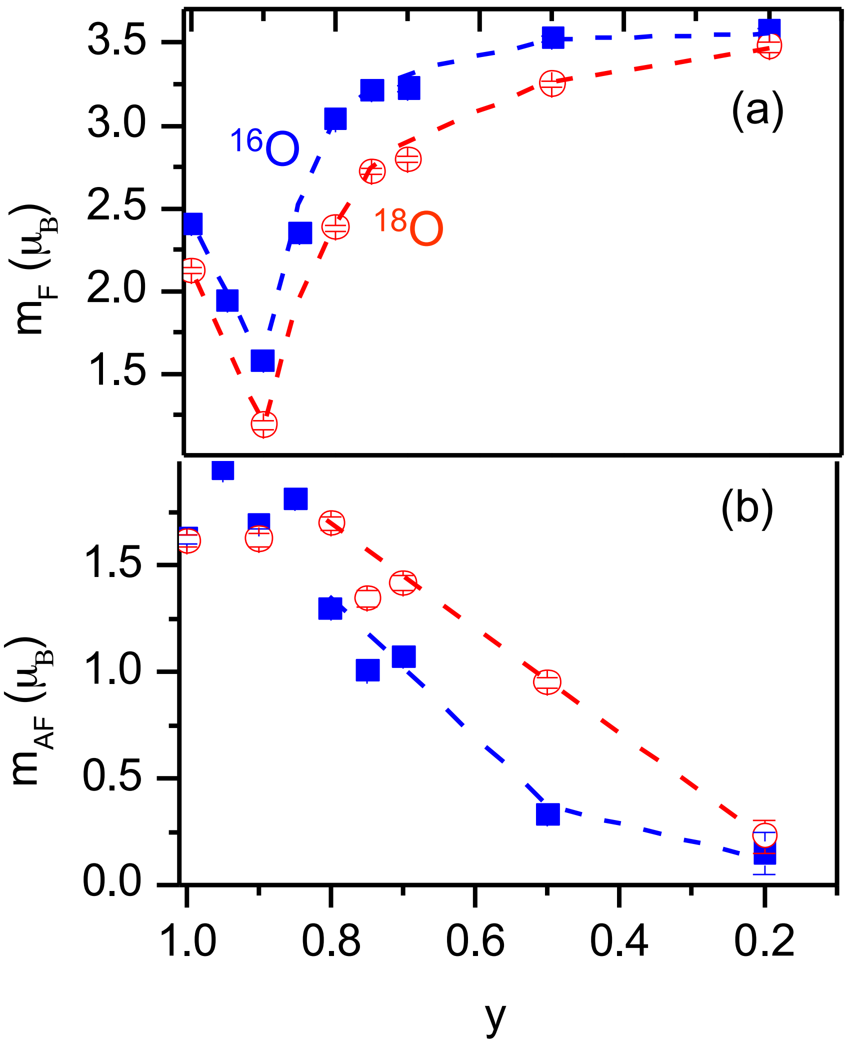

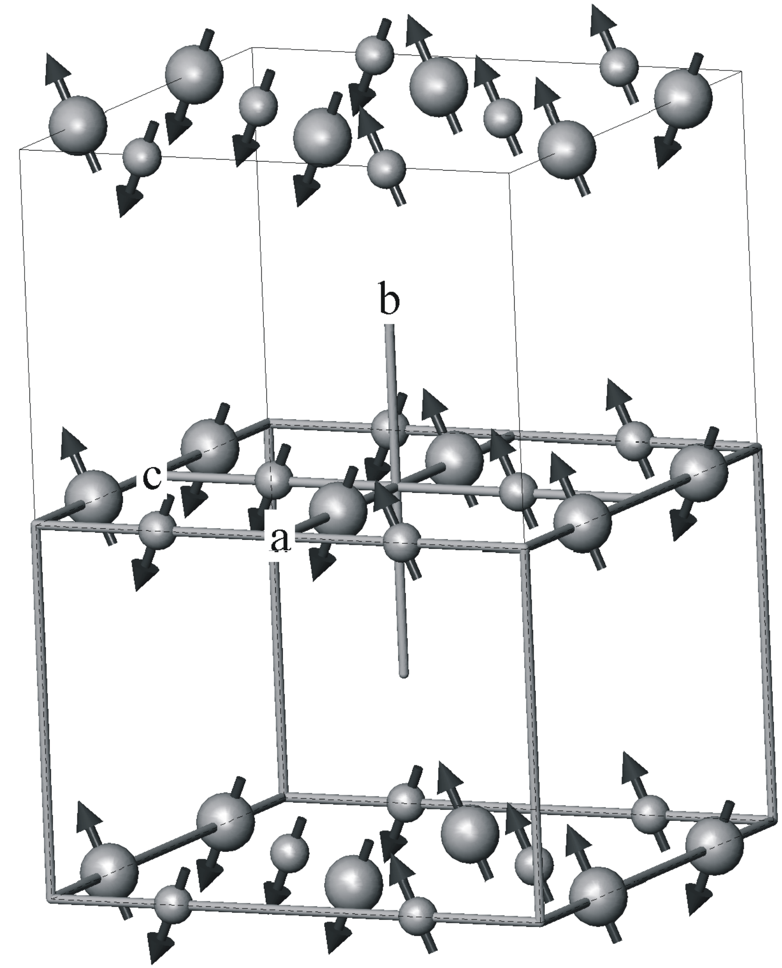

Pseudo CE=PCE: [½ 0 0] and [½ ½ 0]

Magnetic ground state of $(La_{1-y}Pr_y)_{0.7}Ca_{0.3}MnO_3$

Effective magnetic moments = $\sqrt{volume} \bullet moment$

$$\left(\frac{m_A}{M_A}\right)^2 + \left(\frac{m_F}{M_A}\right)^2 = volume = 1$$

$$m_F^2(m_A^2) = M_F^2\left(1 - \frac{m_A^2}{M_A^2}\right)$$

$M_A = 2.26(1)\mu_B$
$M_F = 3.57(2)\mu_B$

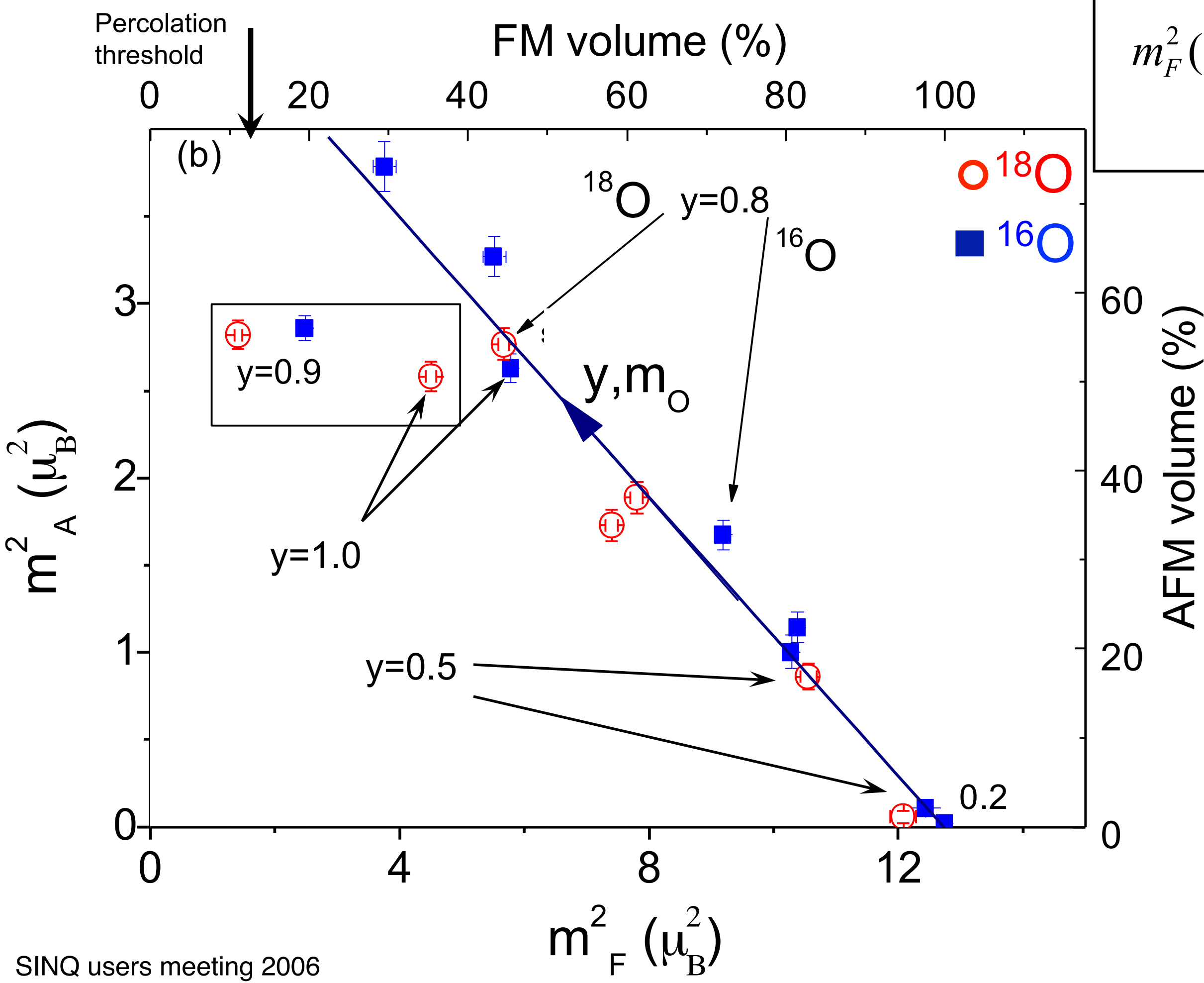

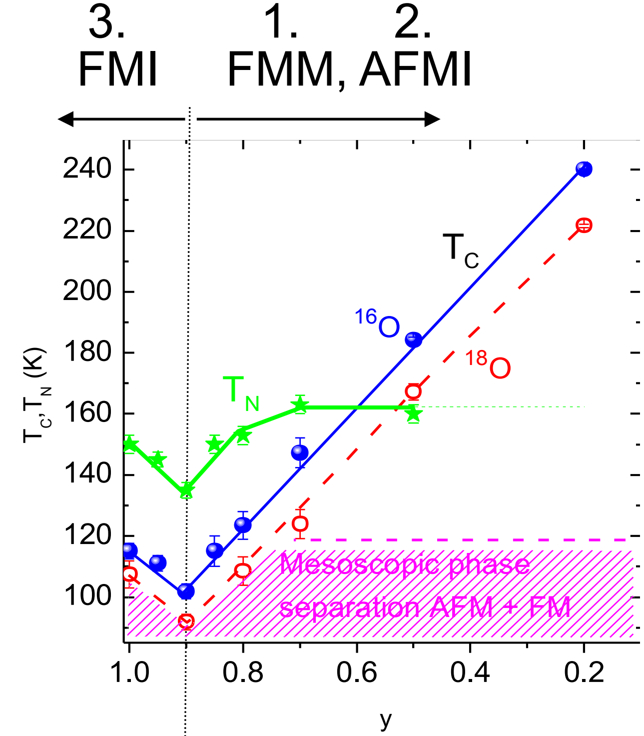

Magnetic ground state of $(La_{1-y}Pr_y)_{0.7}Ca_{0.3}MnO_3$

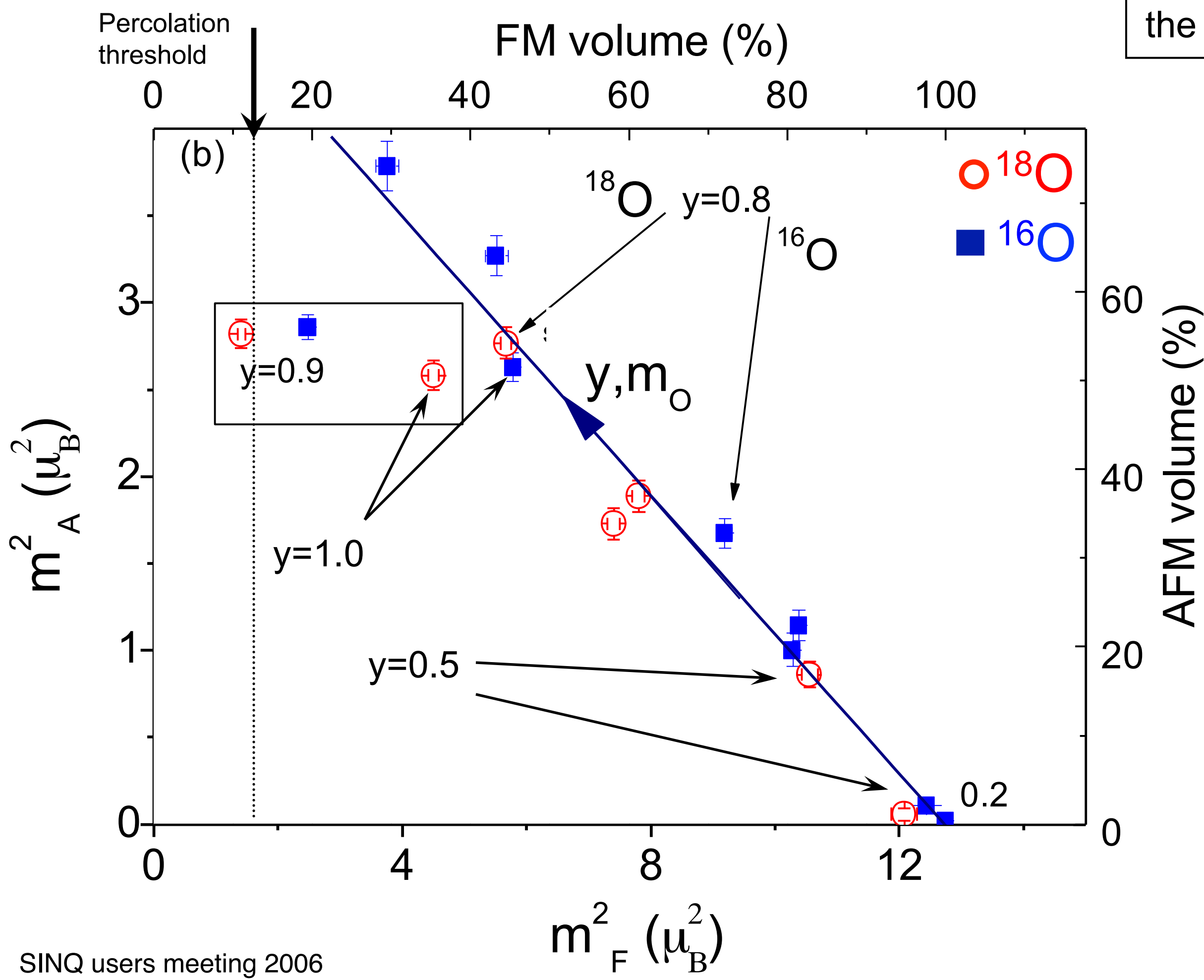

Polaronic narrowing acts as the narrowing due to the increase in *y:*

the phase balance is shifted towards the AFM/CO phase.

Microstrains effect on phase separation

Phase separation is favored by internal micro-strains

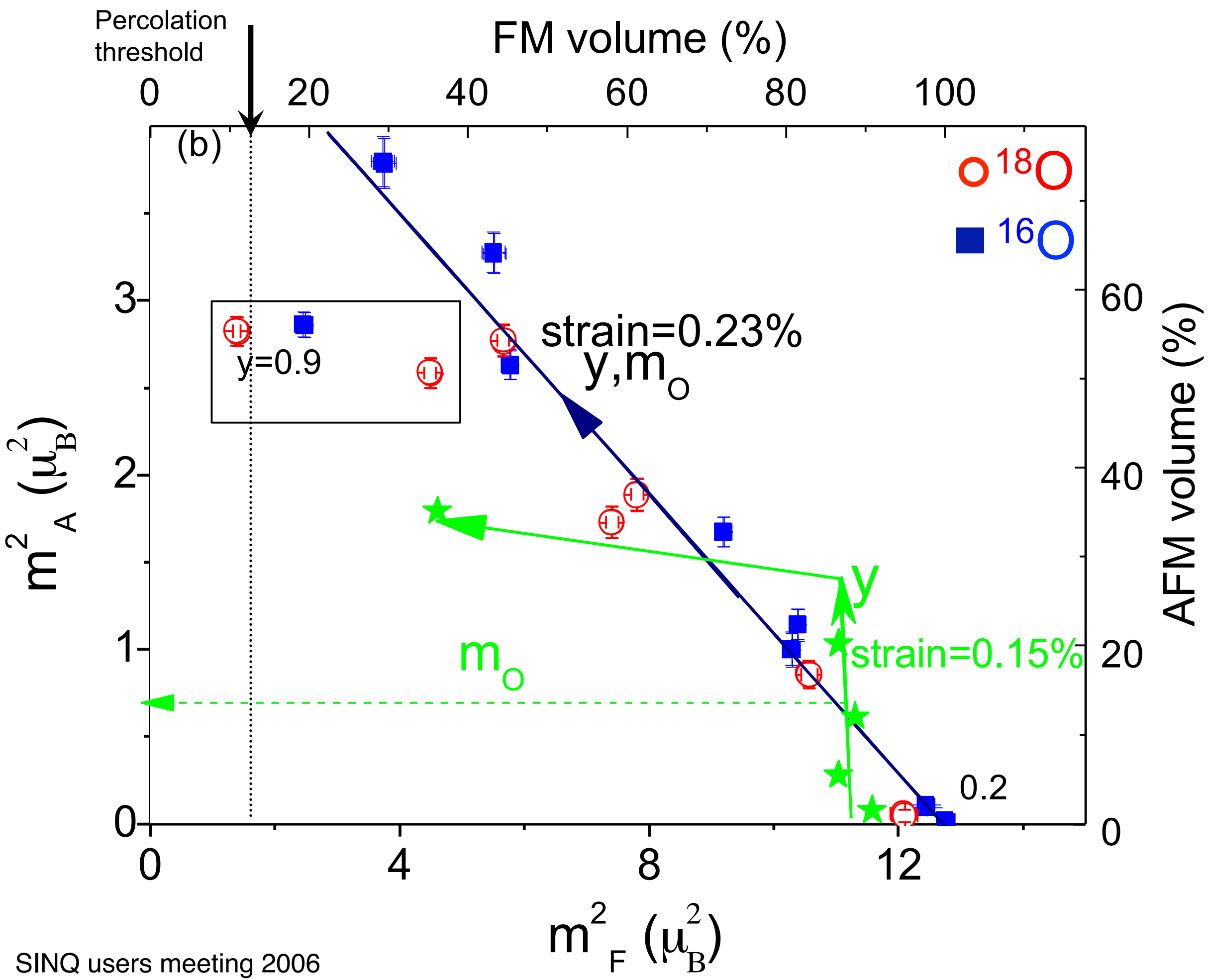

Origin of mesoscopically inhomogeneous state

- ***quenched disorder*** enhances the fluctuation of the competing orders near the original bicritical point [e.g. J.Burgy, A.Moreo, M. Mayr, E.Dagotto et al, PRL, PRB 2000-2004]

- ***lattice distortions*** and the long-range strain similar to one observed at the martensite type structural transition [e.g. K. H. Ahn, T. Lookman, and A. R. Bishop, Nature 428, 401 (2004)]

Suppression of all types of ordering near M-I transition in $(La_{1-y}Pr_y)_{0.7}Ca_{0.3}MnO_3$

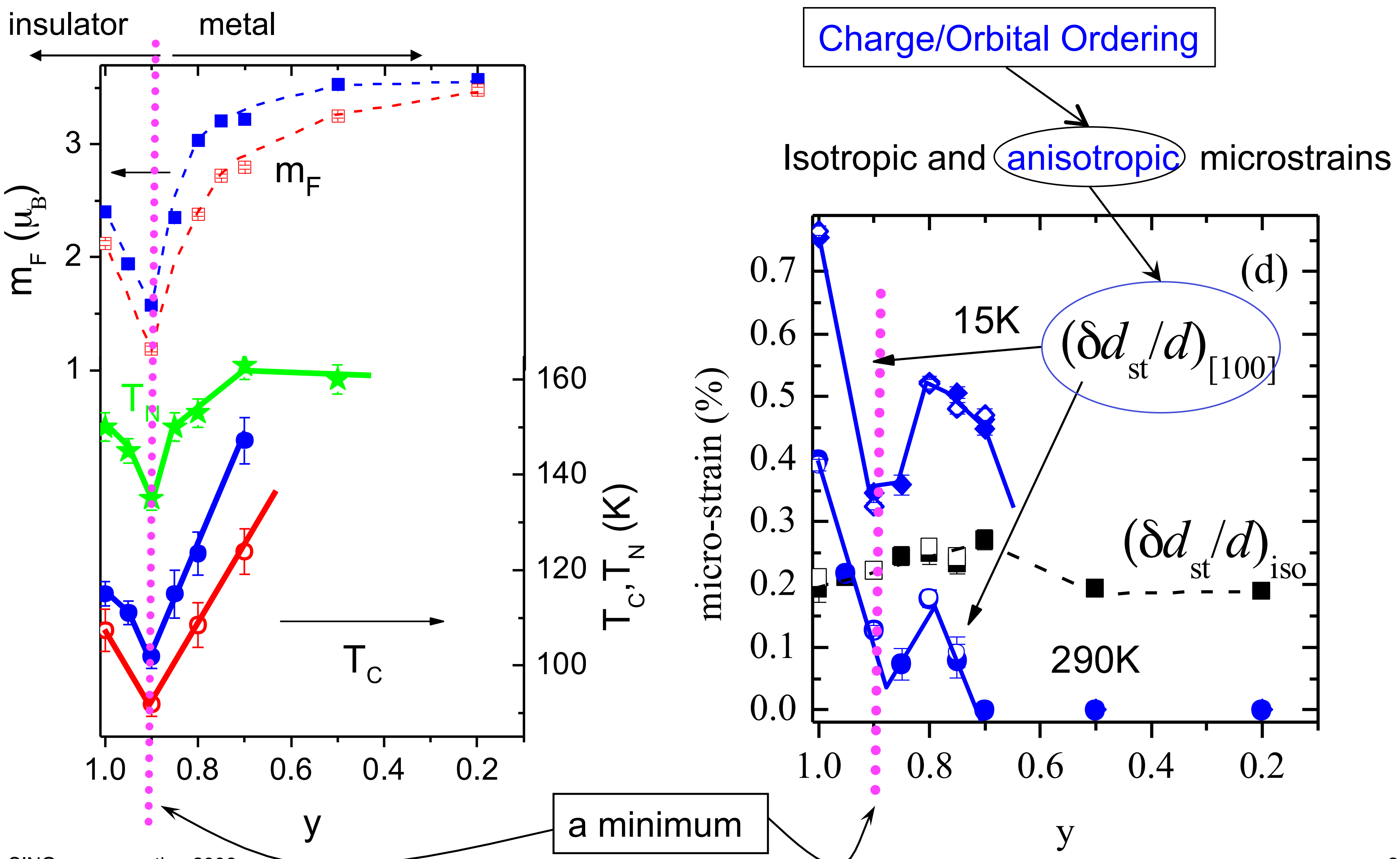

Influence of quenched disorder on the competition between ordered states separated by a first-order transition

J.Burgy, A.Moreo, M. Mayr, E.Dagotto, et al, PRL, PRB 2000-2004

$(La_{1-y}Pr_y)_{0.7}Ca_{0.3}MnO_3$

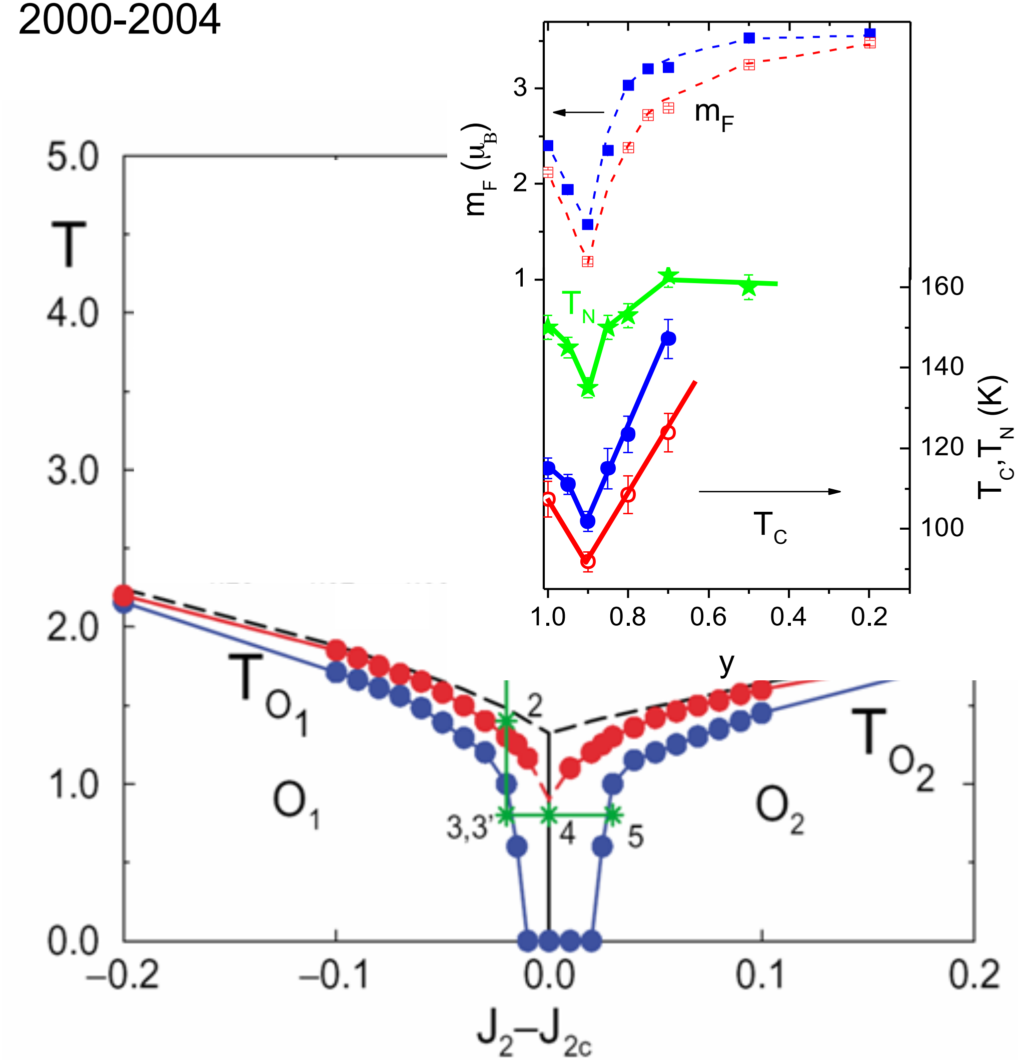

RFIM +correlated disorder

$$H = -J\sum_{\langle ij\rangle} s_i s_j + J'\sum_{[ik]} s_i s_k$$

$J' \rightarrow J'_{ik} = J' + W_{ik}$

α~3 elasticity mechanism of the distortion propagation (Khomskii, Kugel, 2001) $\sim 1/d_{[ik]}^{\ \alpha}$

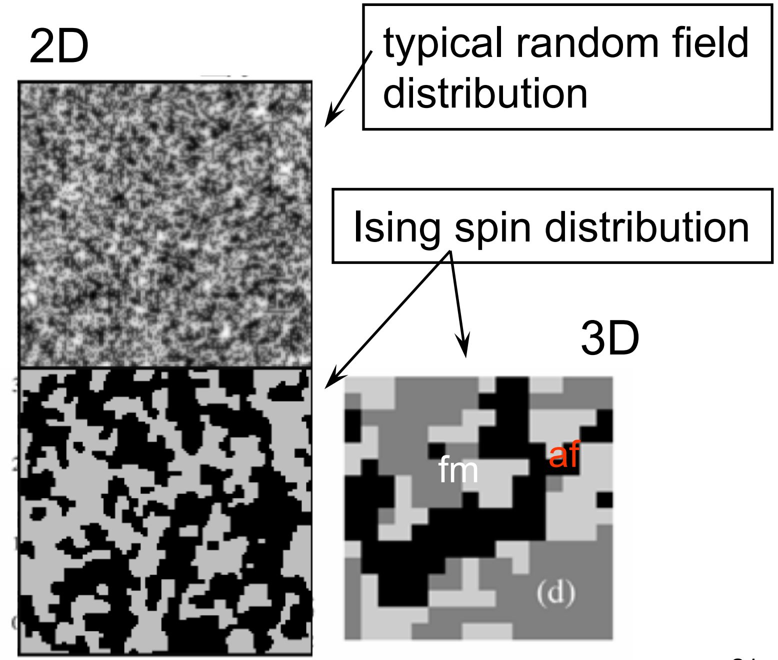

Summary

$(La_{1-y}Pr_y)_{0.7}Ca_{0.3}MnO_3$ (y=0.2-1.0) with ^{16}O/ ^{18}O

- At T=0, there are 3 distinct coexisting mesoscopically phase separated phases: CO/ AFMI + (FMM, FMI)
- the carrier bandwidth (m_O, y) and the crystal lattice micro-strains control the volume fractions of the FM and AFMI clusters.
- quenched disorder is responsible for the formation of the long-scale phase separated state

The End

Samples

Powders of $(La_{1-y}Pr_y)_{0.7}Ca_{0.3}MnO_3$

- **O-series (y=0.2, 0.5, 0.7, 0.75, 0.8, 0.85, 0.9, 0.95 1.0):** by the solid state synthesis from oxides and carbonates of respective metals. The ^{18}O (>85%) samples as well as the final ^{16}O samples were obtained via respective oxygen isotope exchange at the same conditions

- **N-series**[1]: by the "paper" synthesis starting from aqueous solutions of nitrates of the respective metals (N-series) with the final thermal treatment similar to the O-series

[1] Balagurov et al, *Phys. Rev. B* **60**, 383 (1999); *Phys. Rev. B* **64**, 024420-1 (2001); *Eur. Phys. J. B* **19**, 215 (2001)

MO Imaging of Percolative Conduction Paths and Their Breakdown in Phase-Separated $(La_{0.3}Pr_{0.7})_{0.7}Ca_{0.3}MnO_3$

(Faraday effect) magnetization

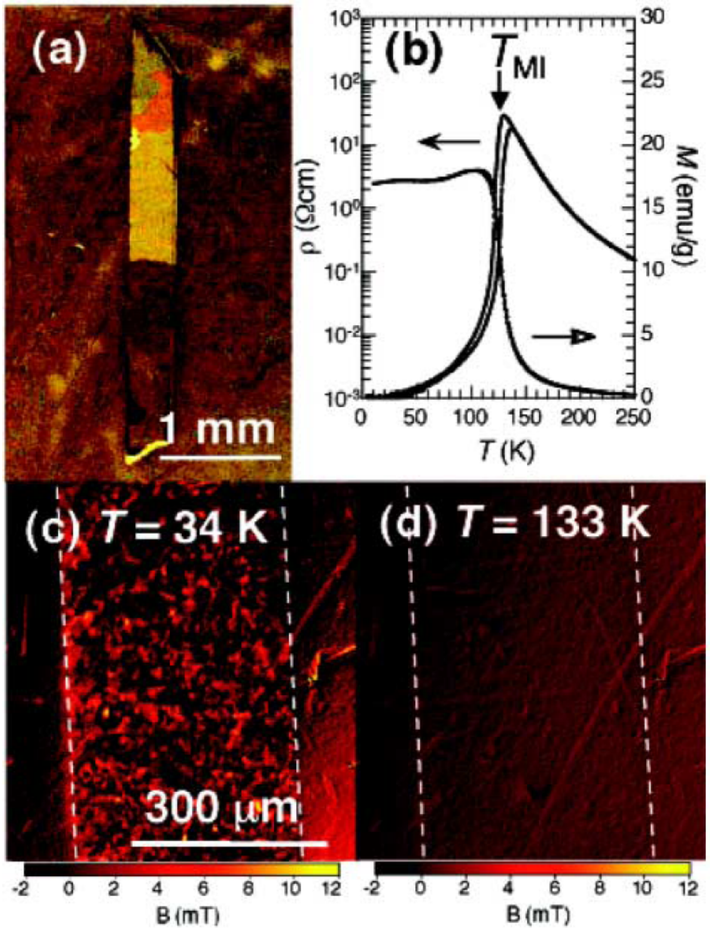

Neutron diffraction

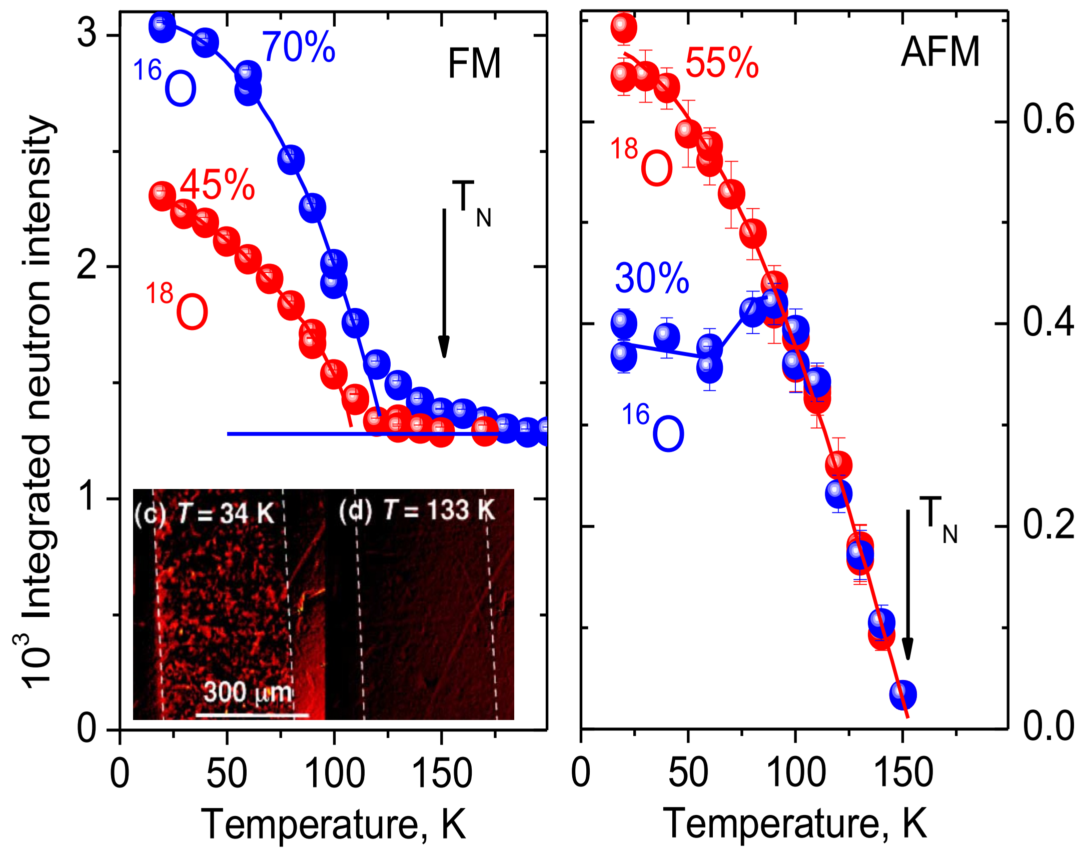

Tokunaga, et al Phys Rev Letters 2004.

Magnetic ordering as a function of temperature

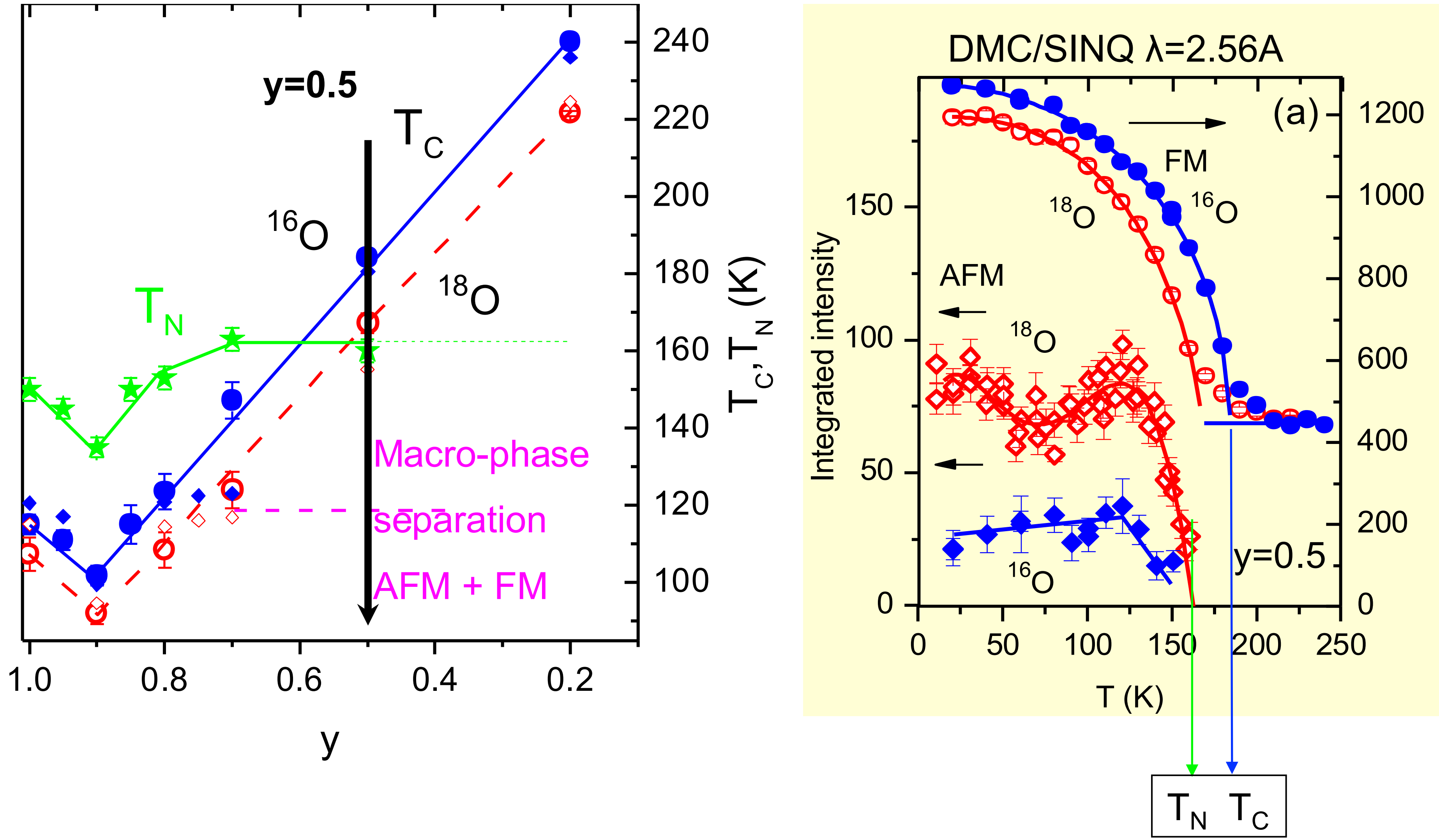

Orbital and Charge ordering

$(La_{1-y}Pr_y)_{0.7}Ca_{0.3}(Mn^{3+})_{0.7}(Mn^{4+})_{0.3}O_3$

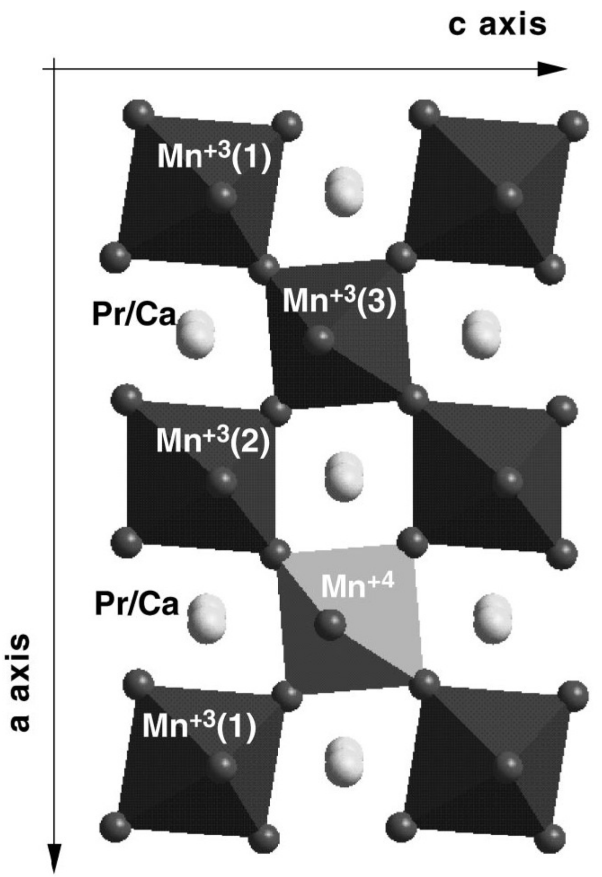

From D.E. Cox et al.,PRB (1998)

- satellite (to *Pnma*) Bragg peaks due to a-axis doubling
- anisotropic (along [100]) peak broadening due to the microstrains
- Mn-O bond length mismatch

Readily observed from NPD data

$(La_{1-y}Pr_y)_{0.7}Ca_{0.3}MnO_3$ phase diagram

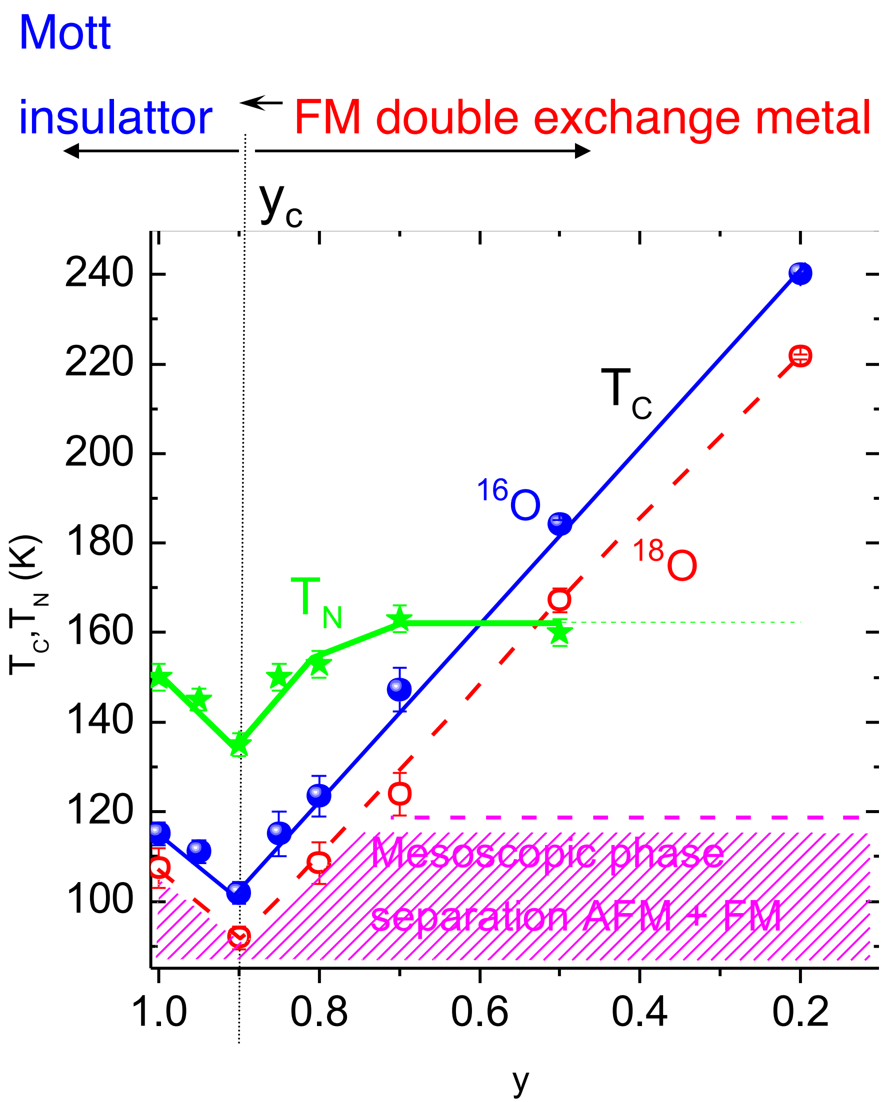

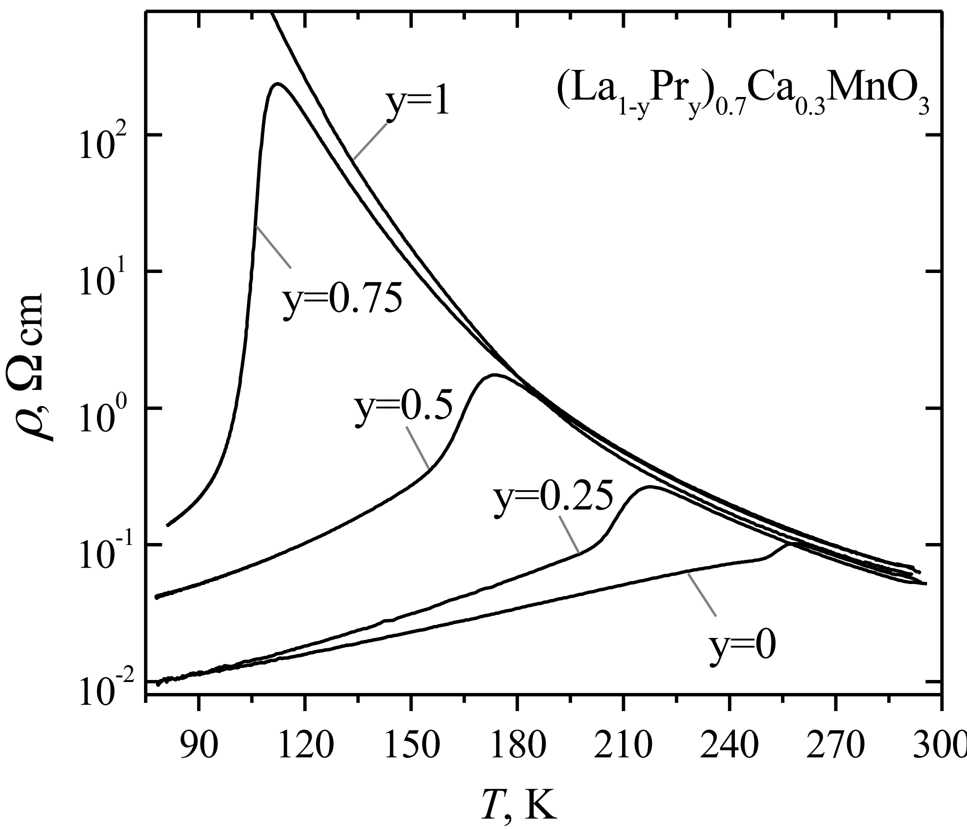

Giant isotope effect in$(La_{1-y}Pr_y)_{0.7}Ca_{0.3}MnO_3$, y=0.75

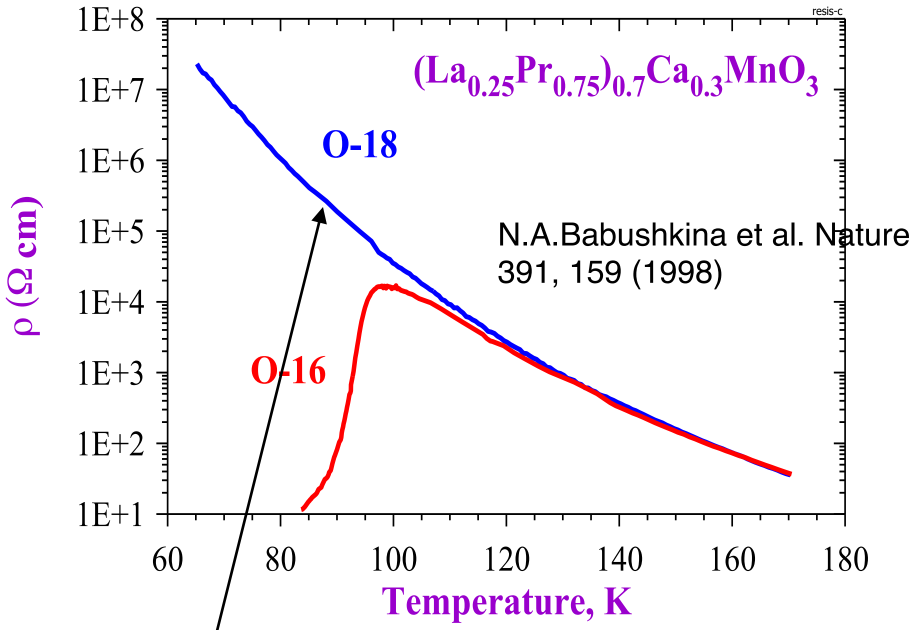

Neutron diffraction intensities

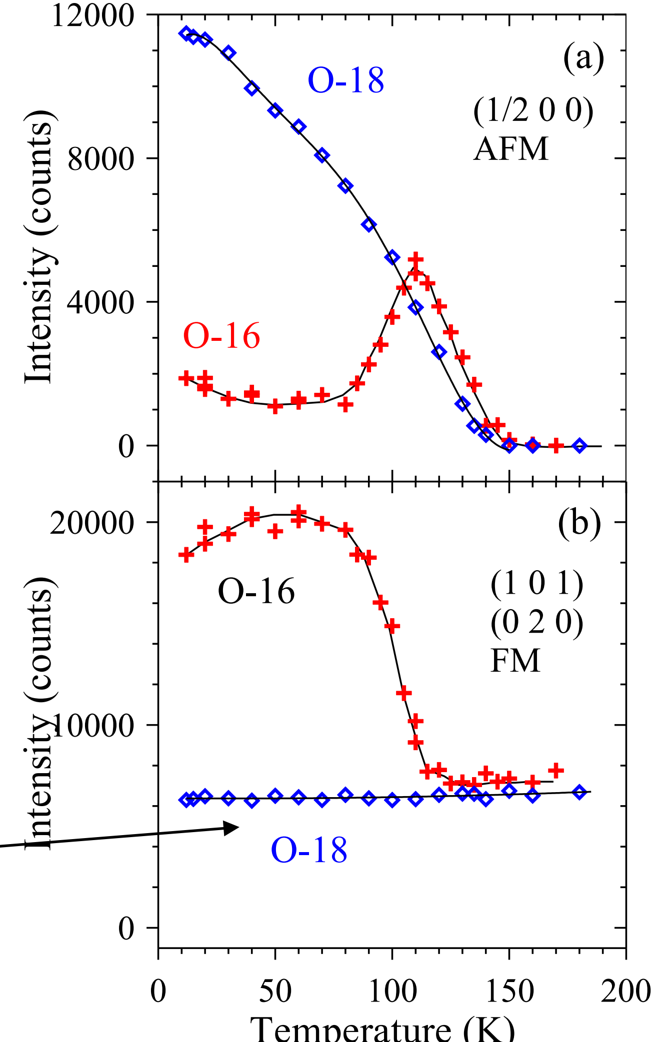

Increase in the m_O leads to complete suppression of the FMM phase and hence to the insulating state

Balagurov et al, *Phys. Rev. B* **60**, 383 (1999); *B* **64**, 24420, (2001)

OO effects

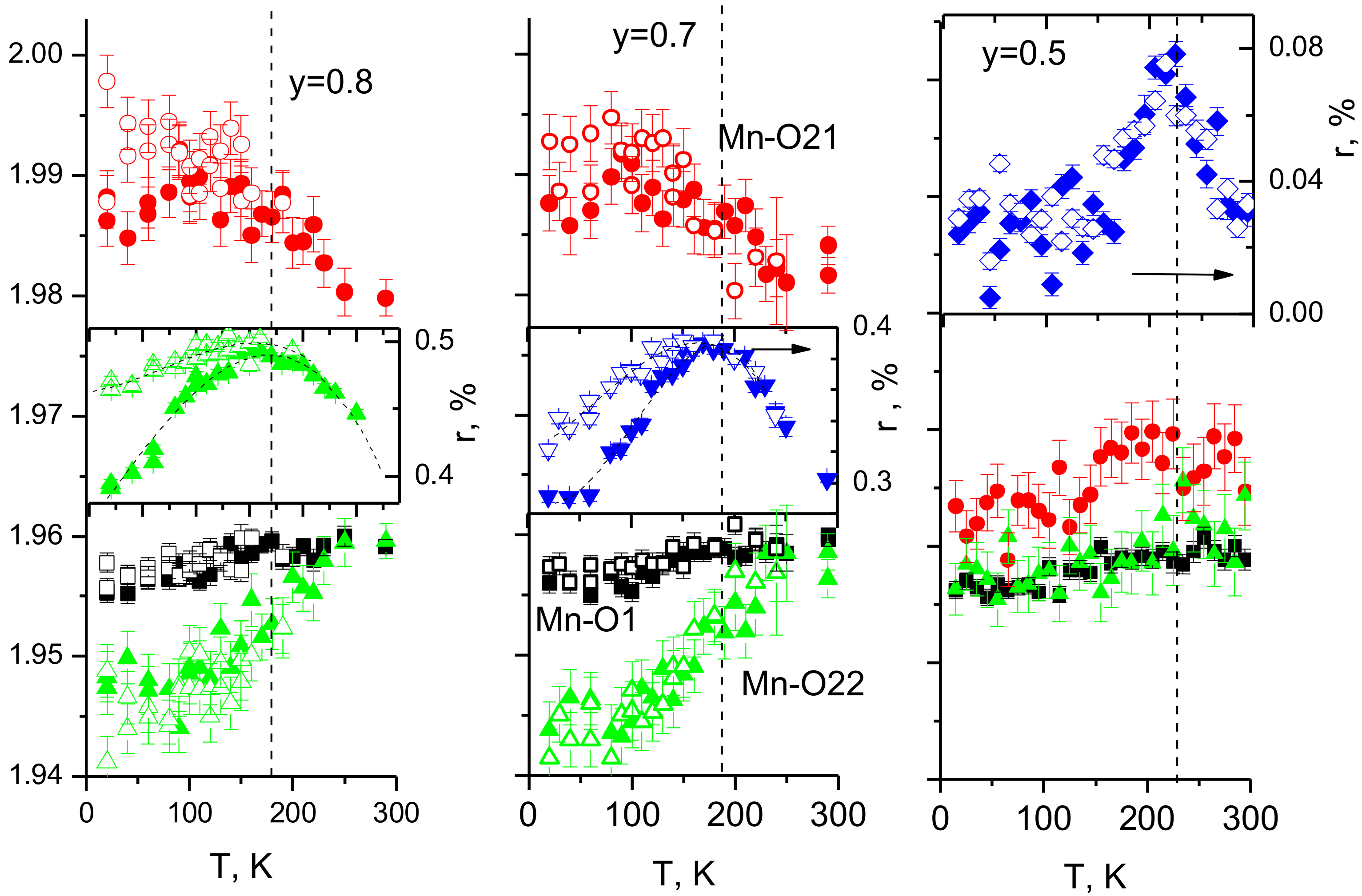

y=0.8
y=0.7
y=0.5
Mn-O21
Mn-O1
Mn-O22
2.00
1.99
1.98
1.97
1.96
1.95
1.94
0.5
0.4
r, %
0.4
0.3
r, %
0.08
0.04
0.00
r, %
0
100
200
300
T, K
T, K
T, K

$(La_{1-y}Pr_y)_{0.7}Ca_{0.3}MnO_3$: $\chi_{ac}(T)=\chi'(T)+i\chi''(T)$

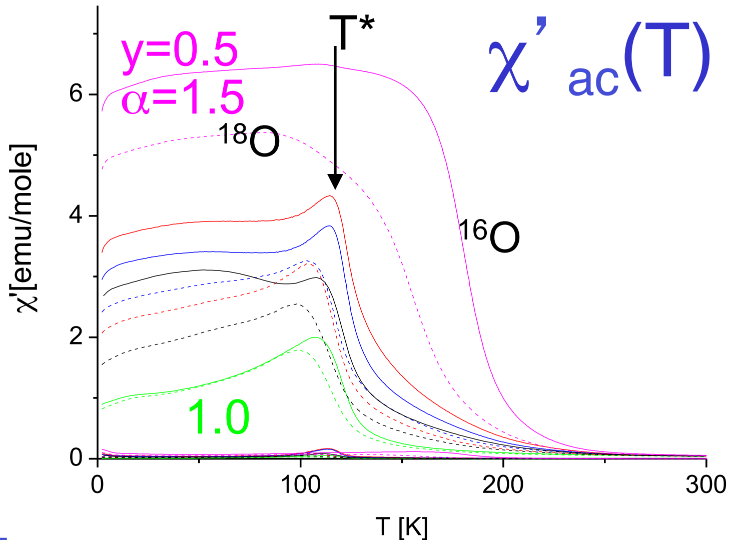

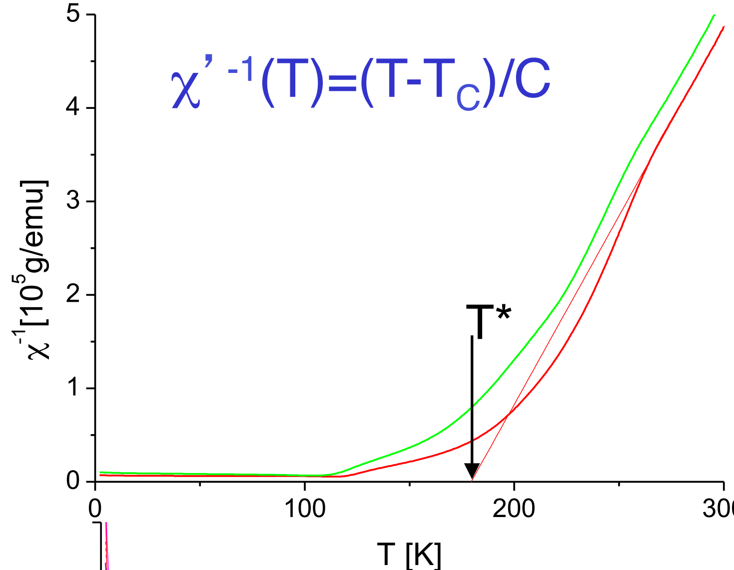

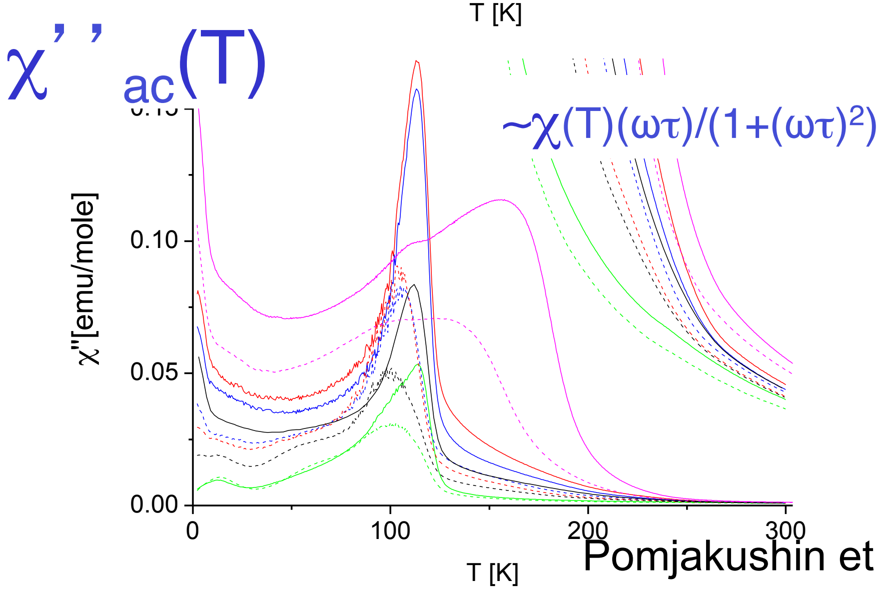

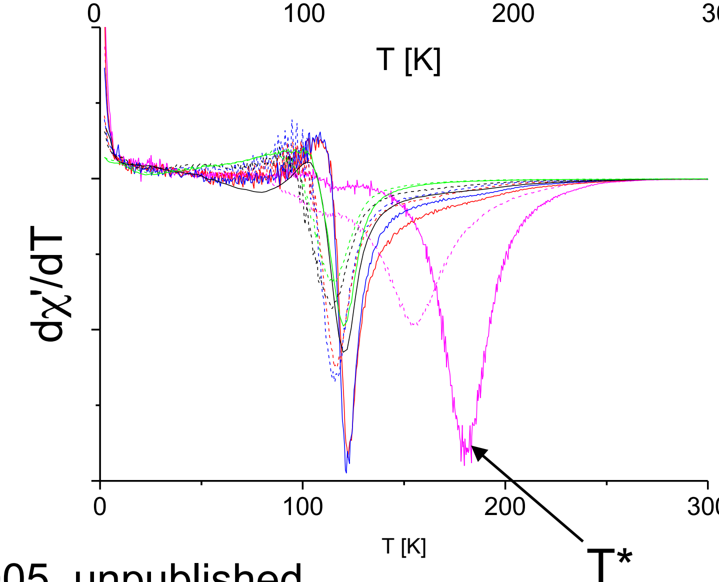

Pomjakushin et al, 2005, unpublished

OO/CO effects (I)

$(La_{1-y}Pr_y)_{0.7}Ca_{0.3}(Mn^{3+})_{0.7}(Mn^{4+})_{0.3}O_3$ $Mn^{3+} : Mn^{4+} = 70:30$

$3t_{2g}1e_g$ $3t_{2g}$

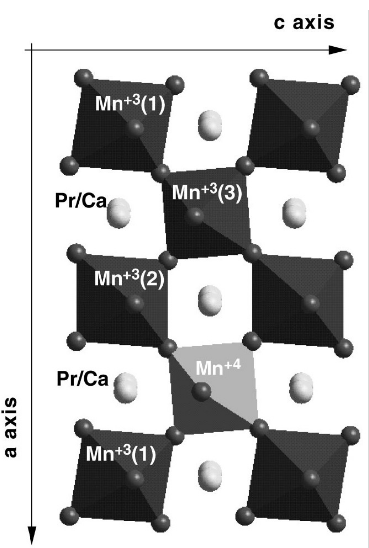

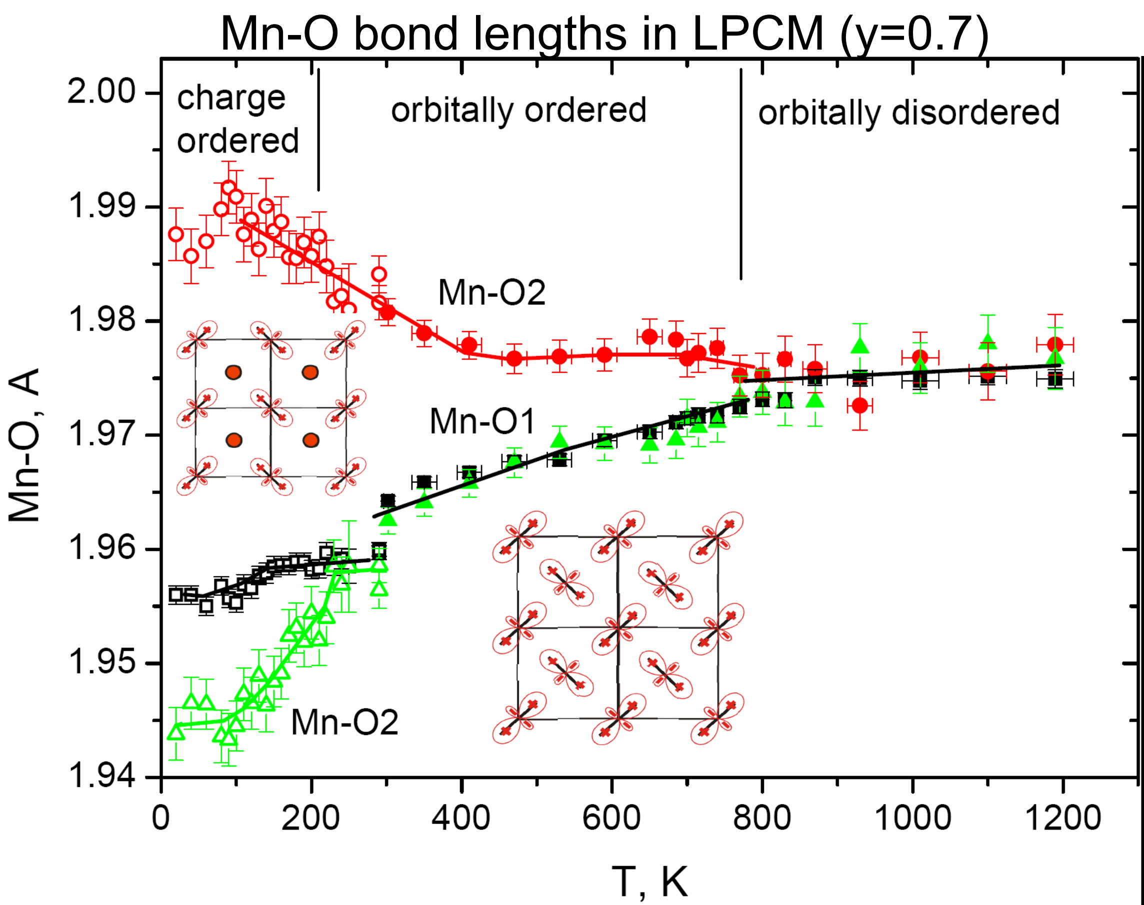

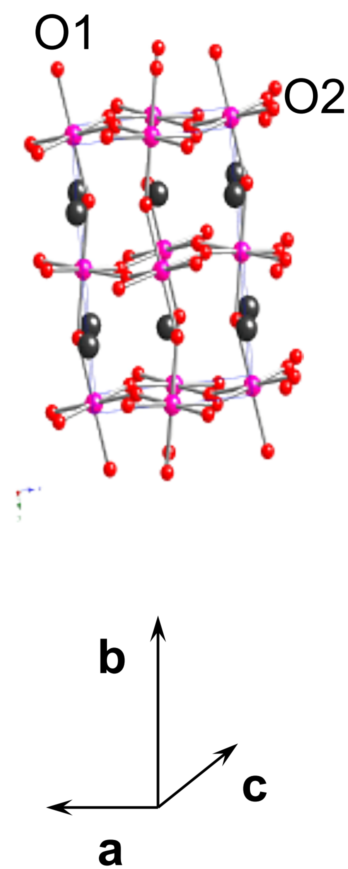

sp.gr. *Pnma*

Deconvolution of the Bragg-peak widths

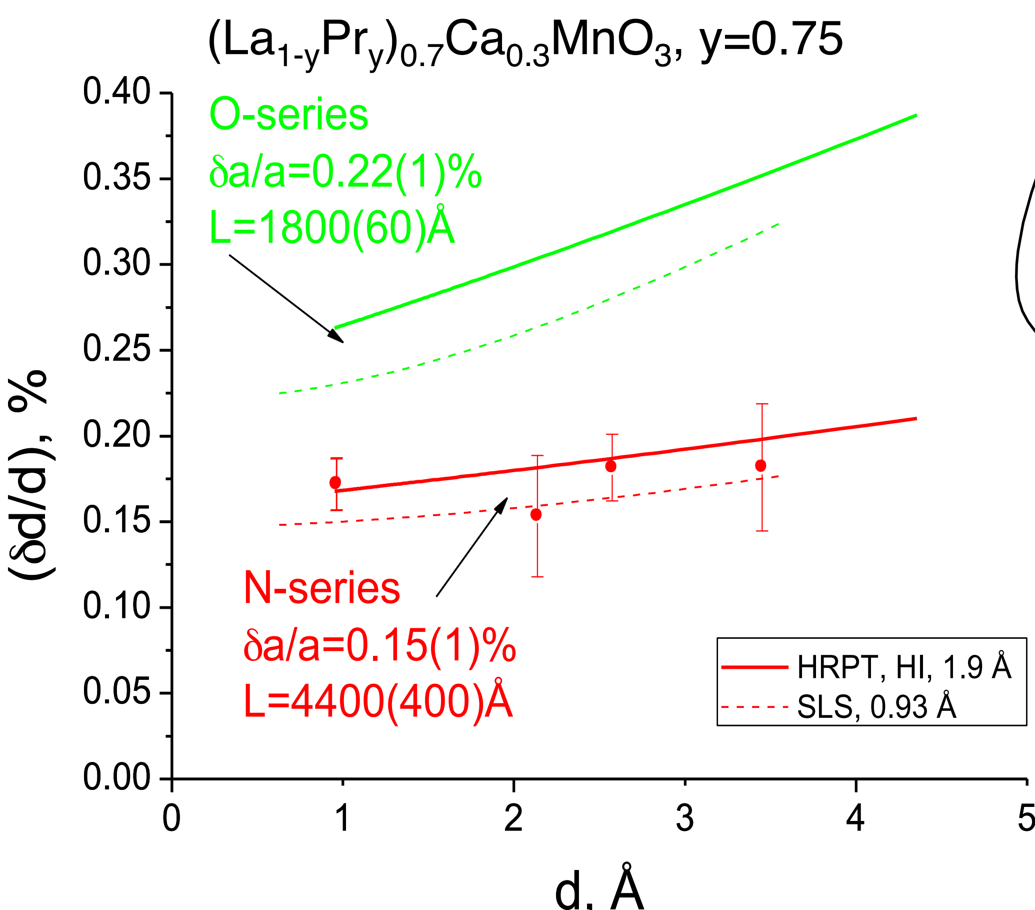

$$I_{\exp} = \int_{-\infty}^{\infty} PV_{sample}(2\theta - \xi) PV_{instrument}(\xi) d\xi$$

Deconvolution of the pseudo-Voigt Bragg peaks width δ(2θ)="*Cagliotti*" with the instrument resolution function.

<u>Bragg peak width</u>

δd/d= δa/a ⊗ d/L

strain size

PV=Pseudo-Voigt

Gaussian ⊗ Lorenzian

$$\int_{-\infty}^{\infty} G(2\theta - \xi) L(\xi) d\xi$$

T-dep of anisotropic strain

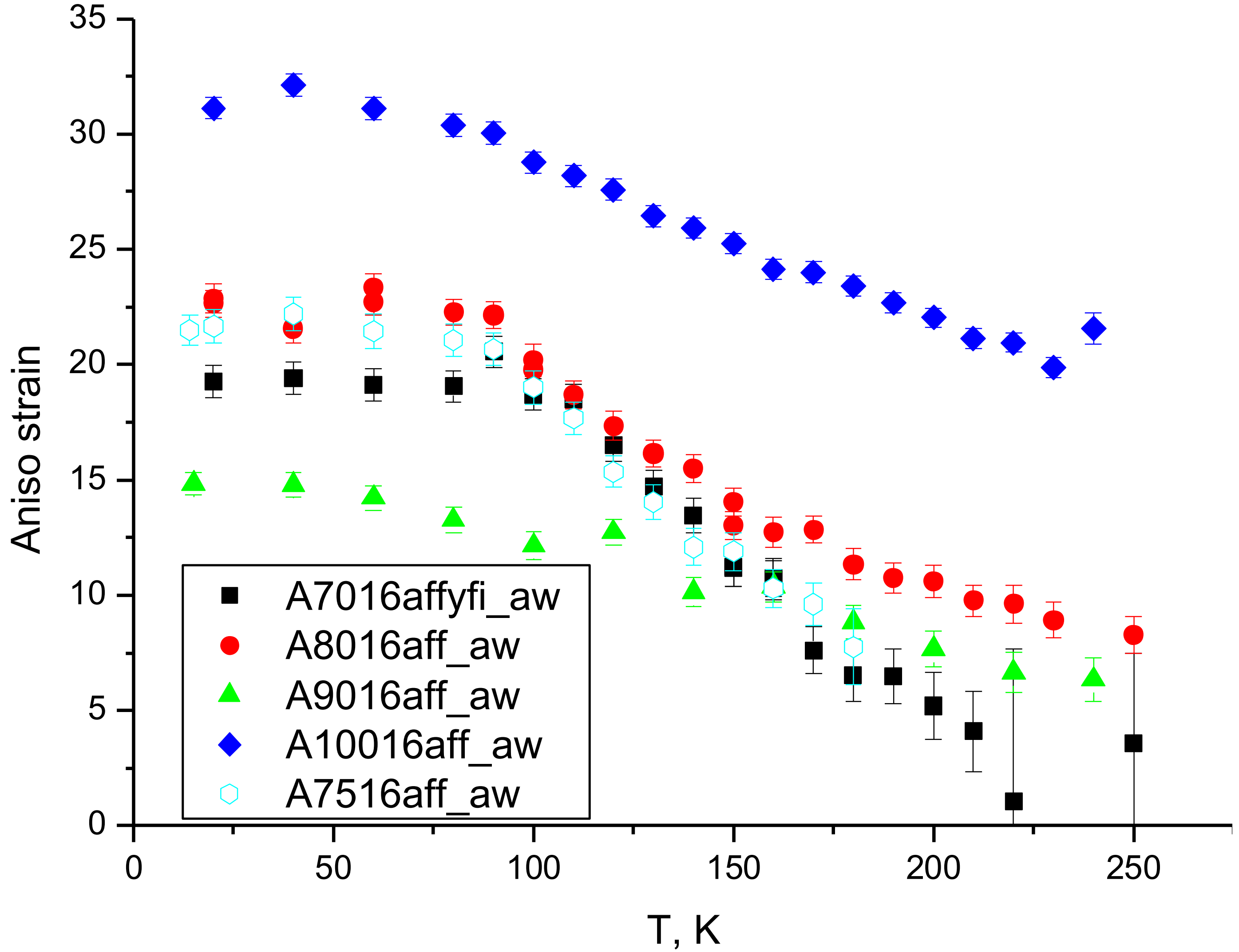

Thermal displacement parameters

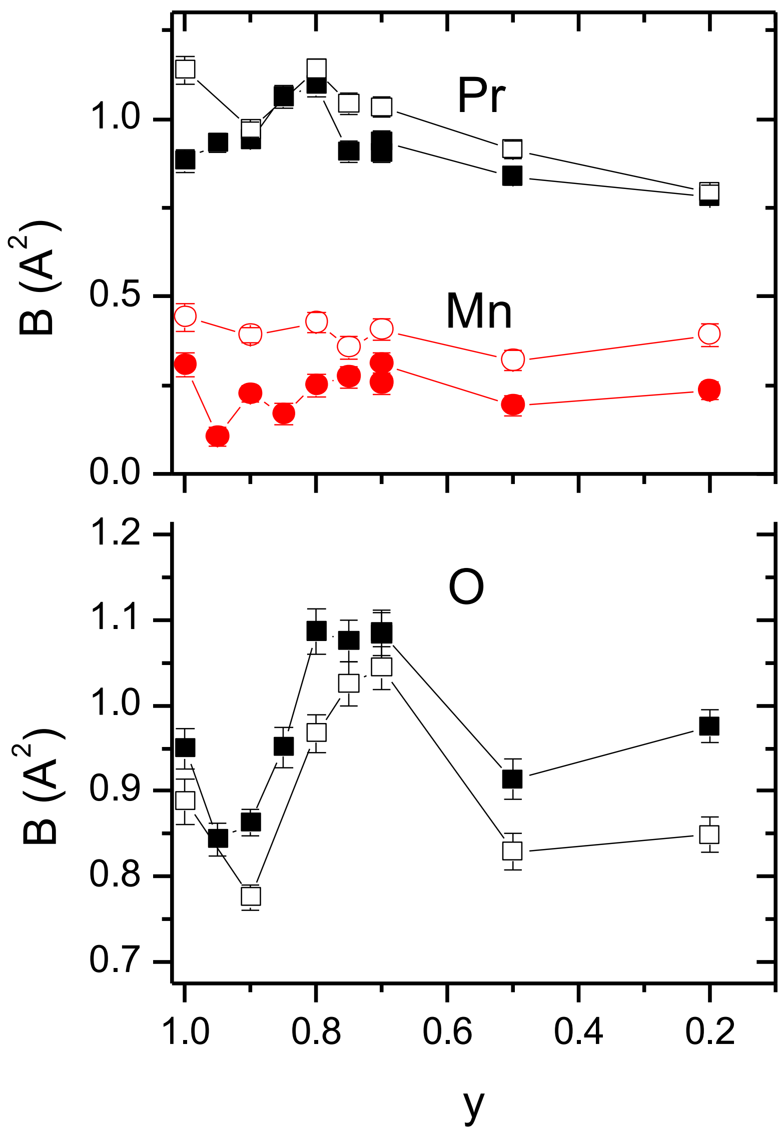

$B^{1/2} \sim T <1/\omega^2> 1/M$

a,b,c

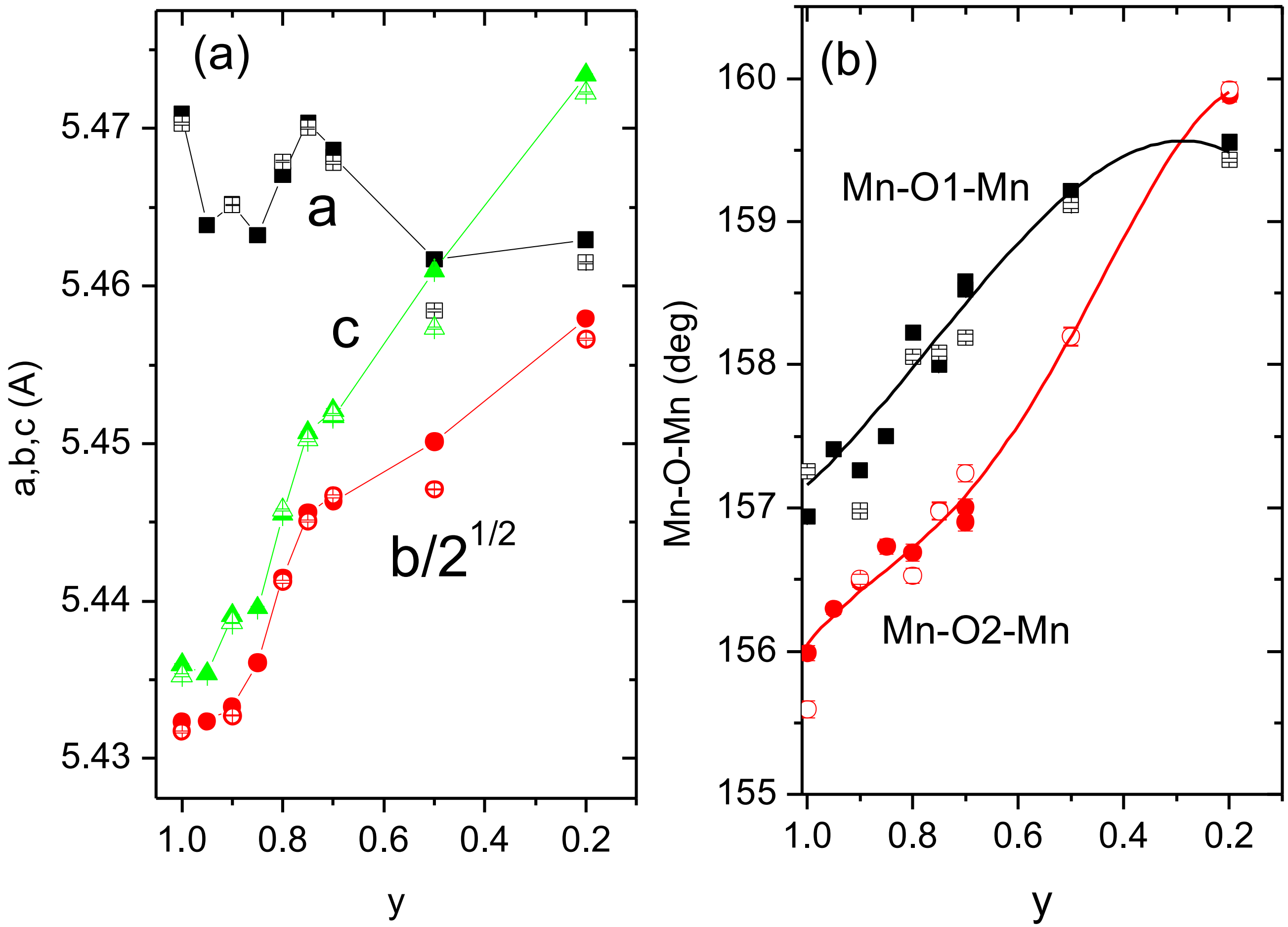
(a)
a
c
$b/2^{1/2}$
5.47
5.46
5.45
5.44
5.43
a,b,c (A)
1.0
0.8
0.6
0.4
0.2
y
(b)
Mn-O1-Mn
Mn-O2-Mn
160
159
158
157
156
155
Mn-O-Mn (deg)
1.0
0.8
0.6
0.4
0.2
y

Magnetic state. Bragg I(T)

x=0.8, 0.75. “New” O-series

x=0.75. “Old” N-series

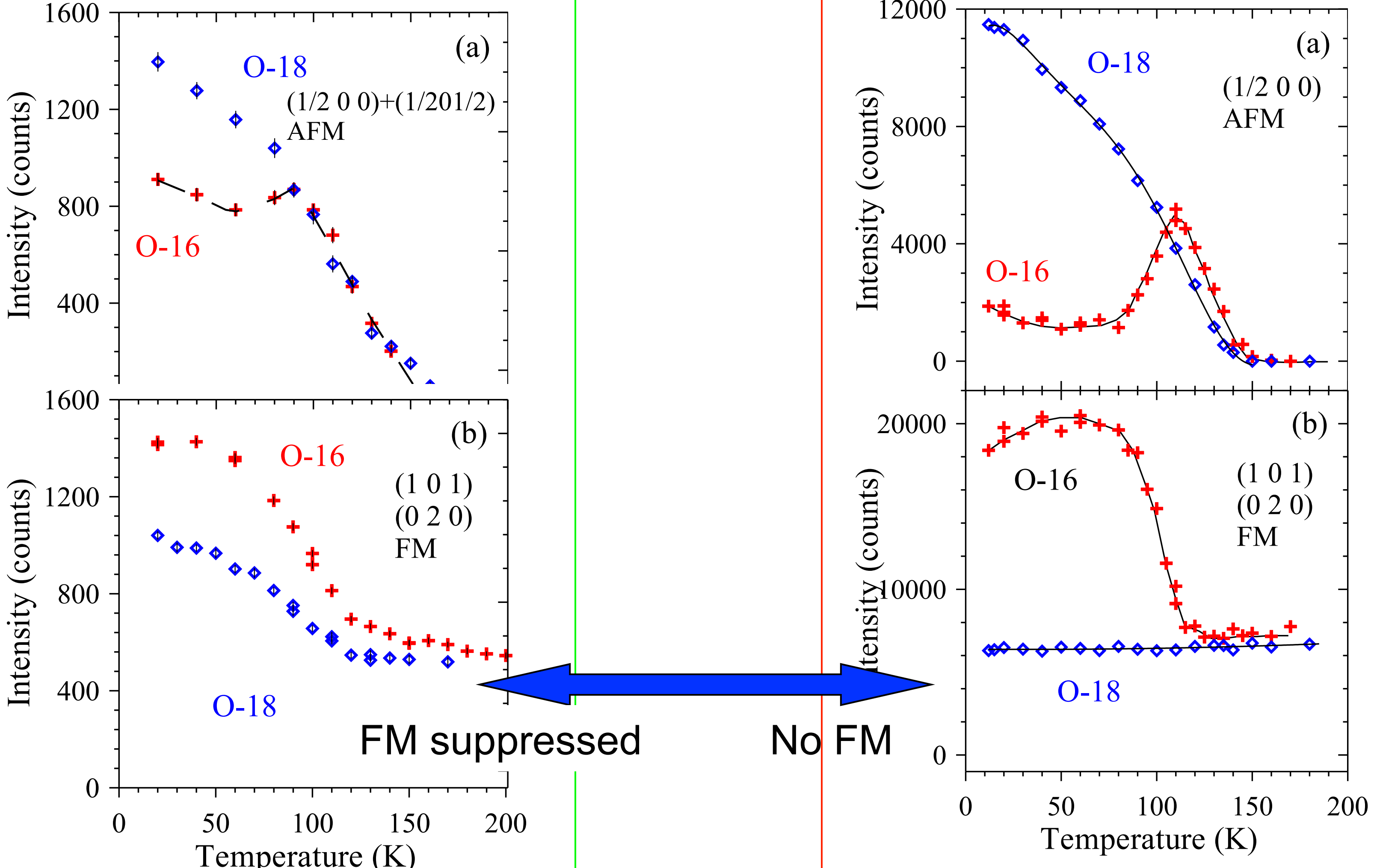

Saturated effective magnetic moments in $(La_{1-y}Pr_y)_{0.7}Ca_{0.3}MnO_3$

"New" O-series

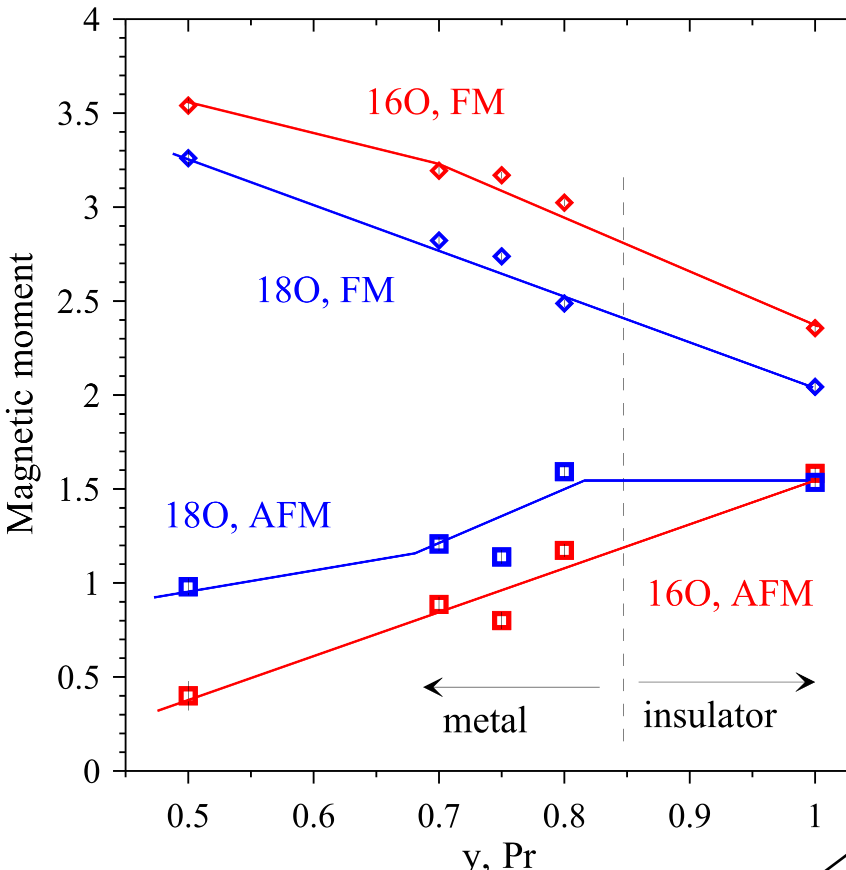

Metallic FM+AFM separated state

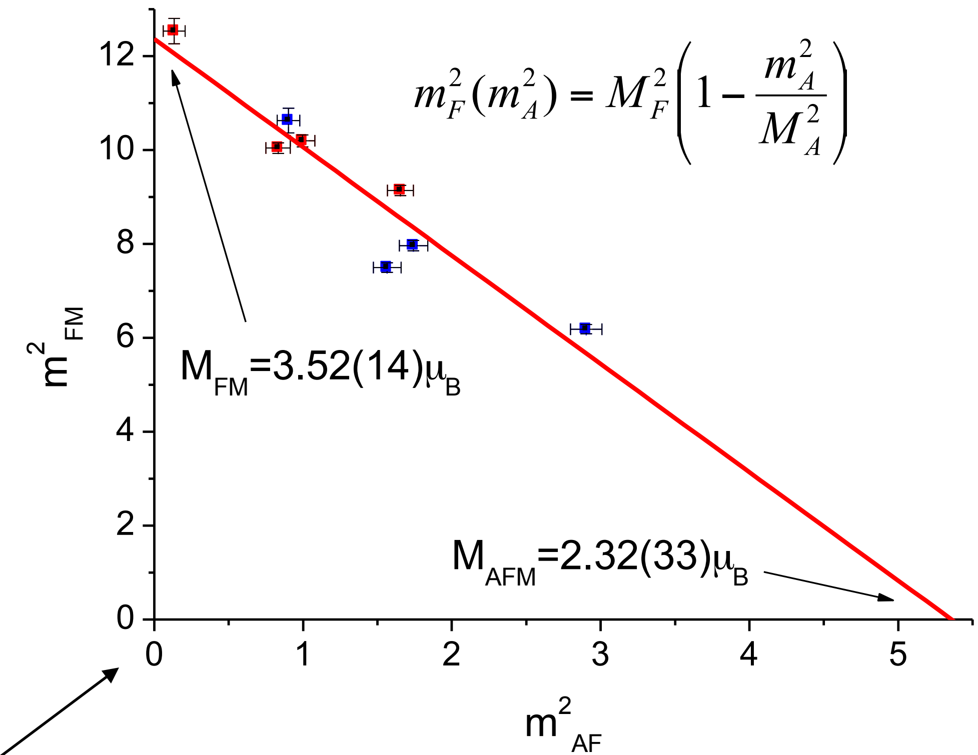

Effective moments

$$\begin{cases} m_{AF} = \nu^{1/2} M_{AF} \\ m_F = (1-\nu)^{1/2} M_F \end{cases}$$

Volume fraction

Saturated effective magnetic moments in $(La_{1-y}Pr_y)_{0.7}Ca_{0.3}MnO_3$

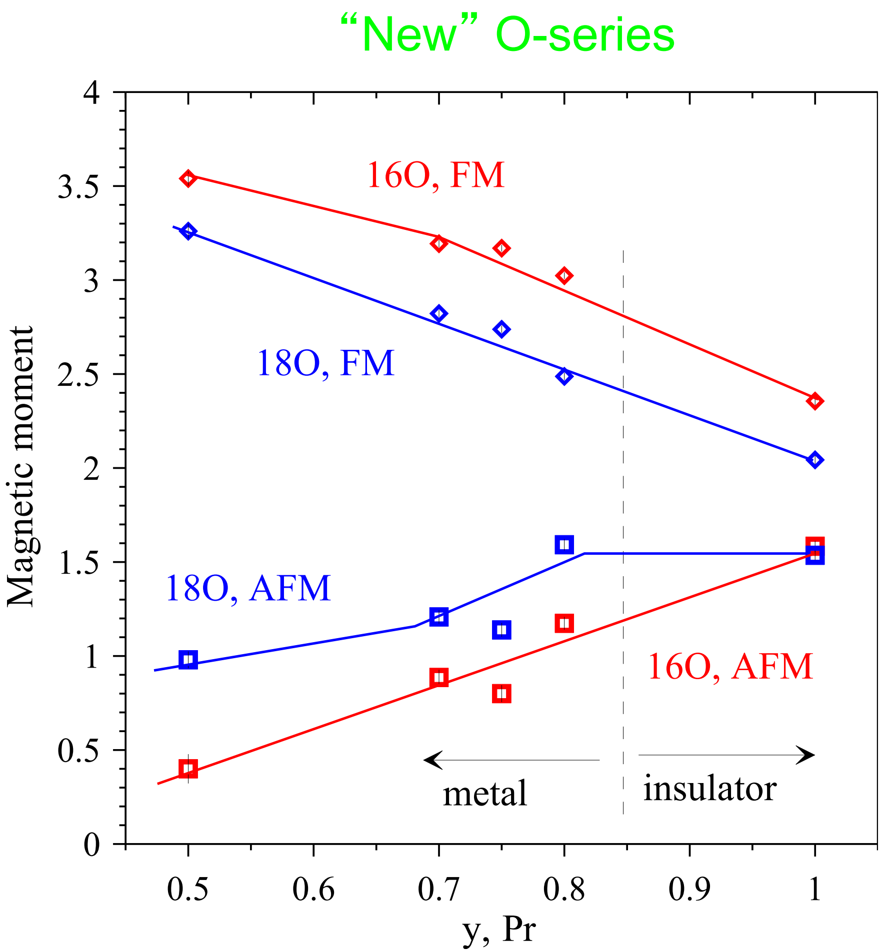

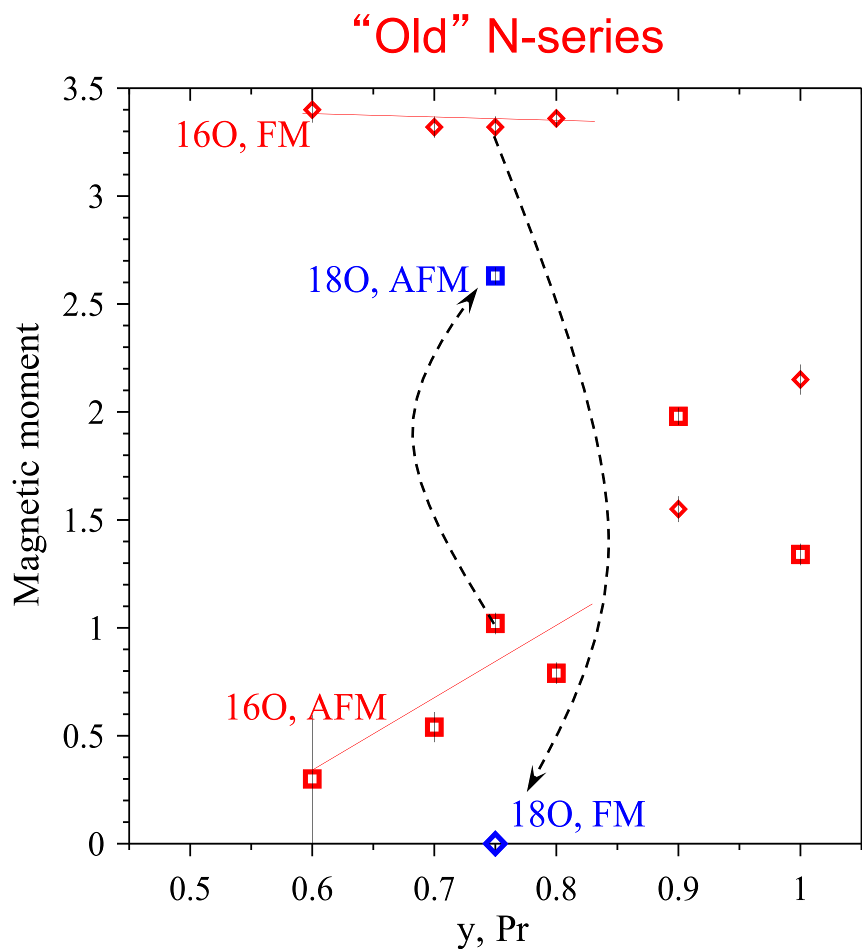

Effective moments

$$\begin{cases} m_{AF} = \nu^{1/2} M_{AF} \\ m_F = (1-\nu)^{1/2} M_F \end{cases}$$

Volume fraction

What is the difference between two series? Crystal structure?

$(La_{1-y}Pr_y)_{0.7}Ca_{0.3}MnO_3$, y=0.75 from both N- and O-series
Pnma, single phase at 290K

SLS X-ray material beamline.
Ultra-high resolution. λ=0.9A

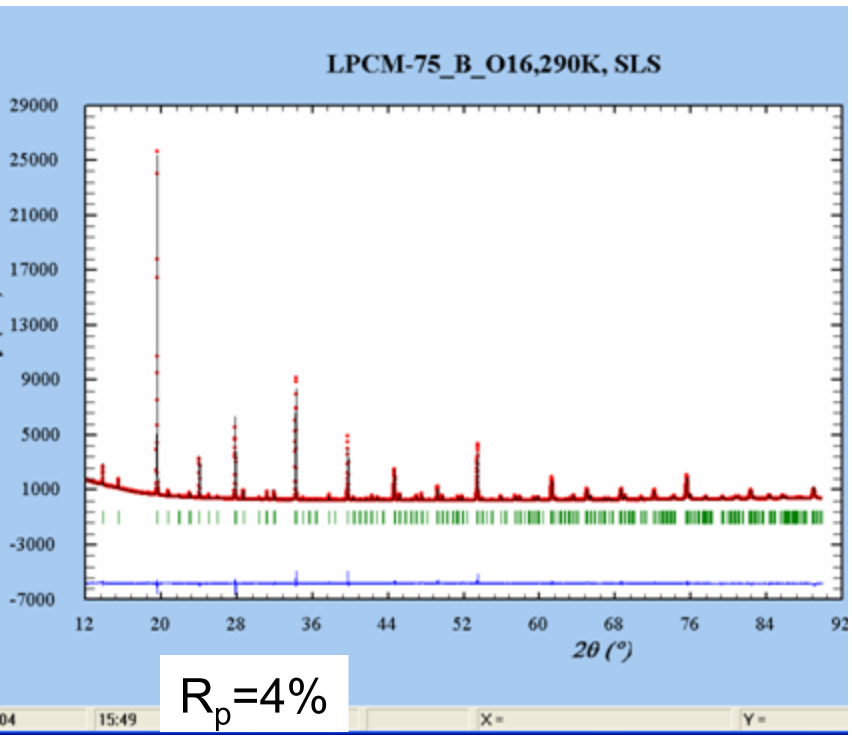

R_p=4%

HRPT/SINQ diffraction pattern.
λ=1.9A, HI-mode

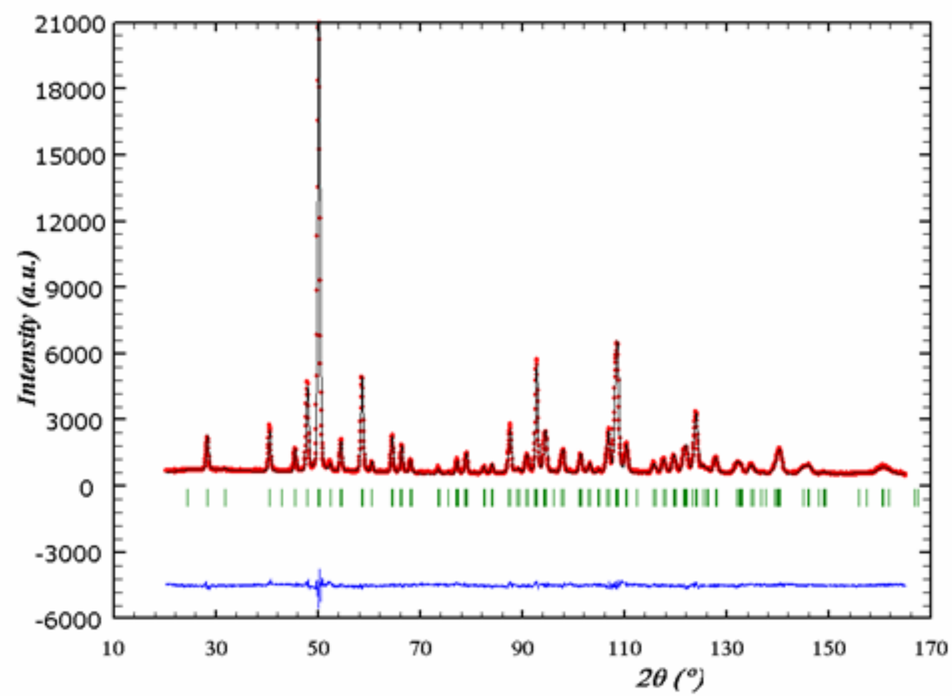

R_p=3.4%, χ^2=3

Comparison of lattice parameters

Pnma

$(La_{1-y}Pr_y)_{0.7}Ca_{0.3}MnO_3$,

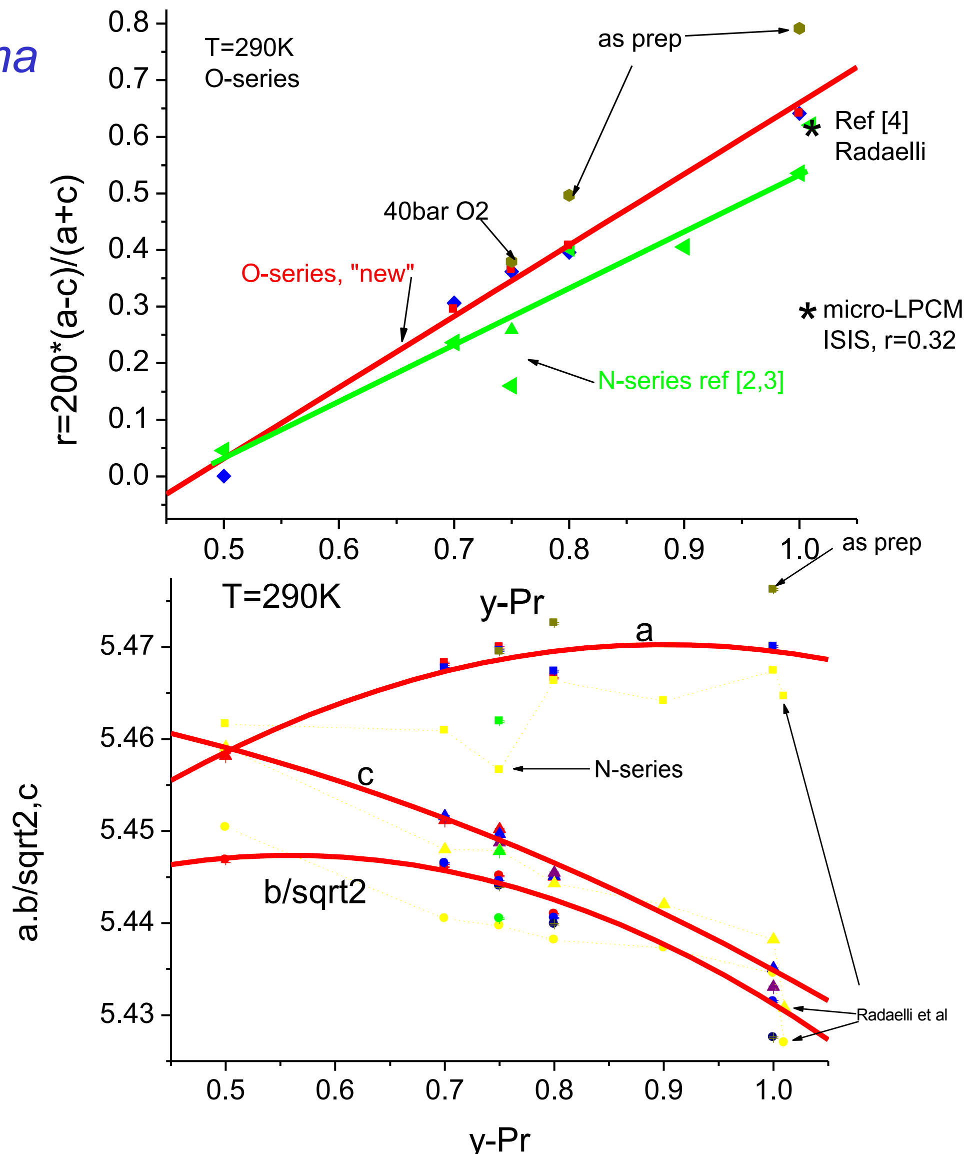

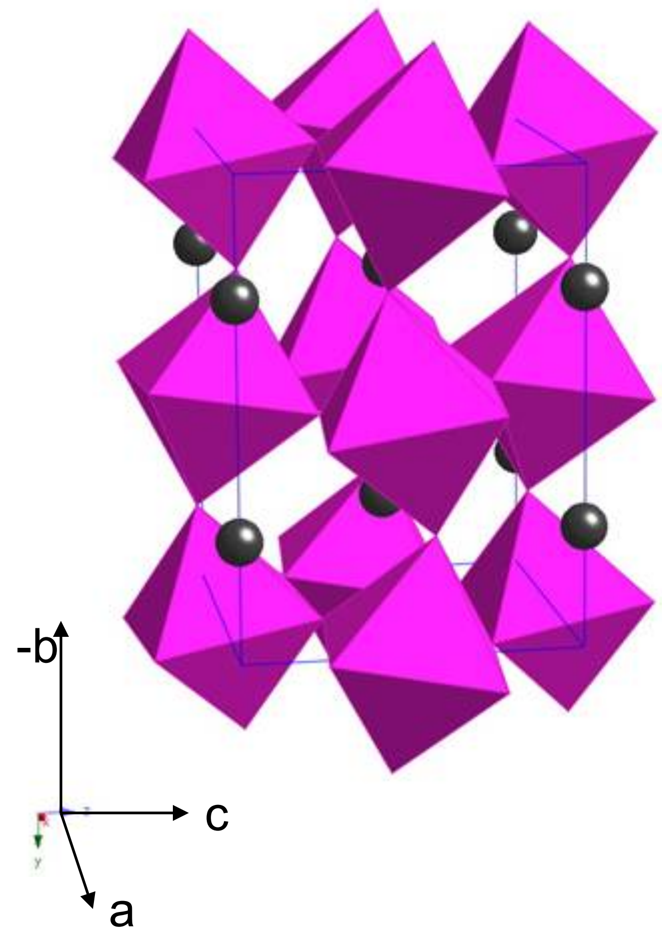

Bragg peak widths. Synchrotron X-ray, HRPT

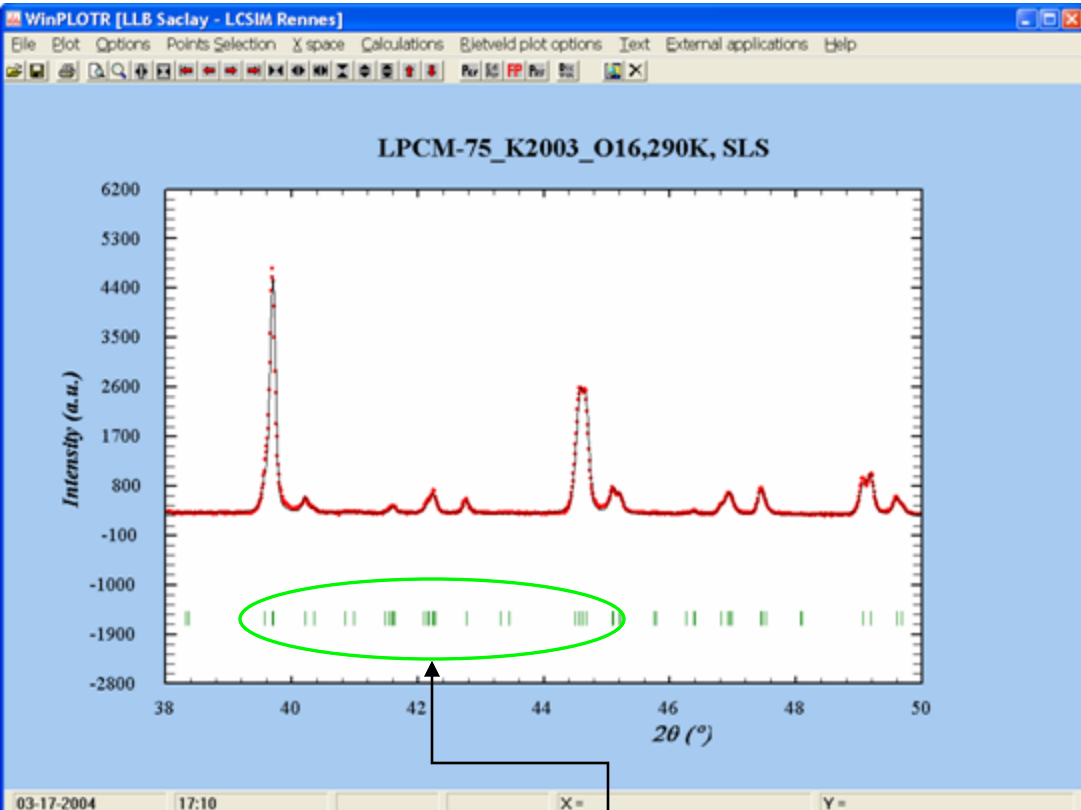

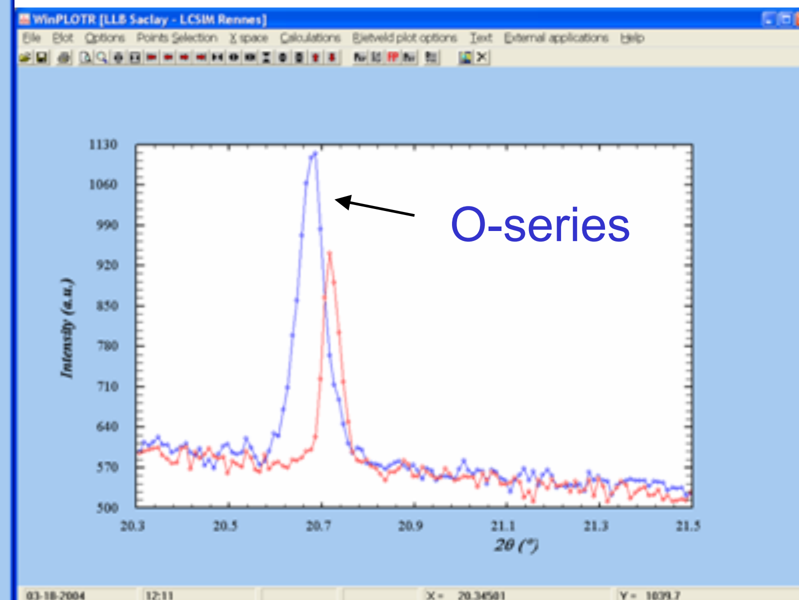

Pseudo-cubic metrics:
Strong peak overlap

Deconvolution of the Bragg-peak widths. Comparison of HRPT and synchrotron

$(La_{1-y}Pr_y)_{0.7}Ca_{0.3}MnO_3$, y=0.75

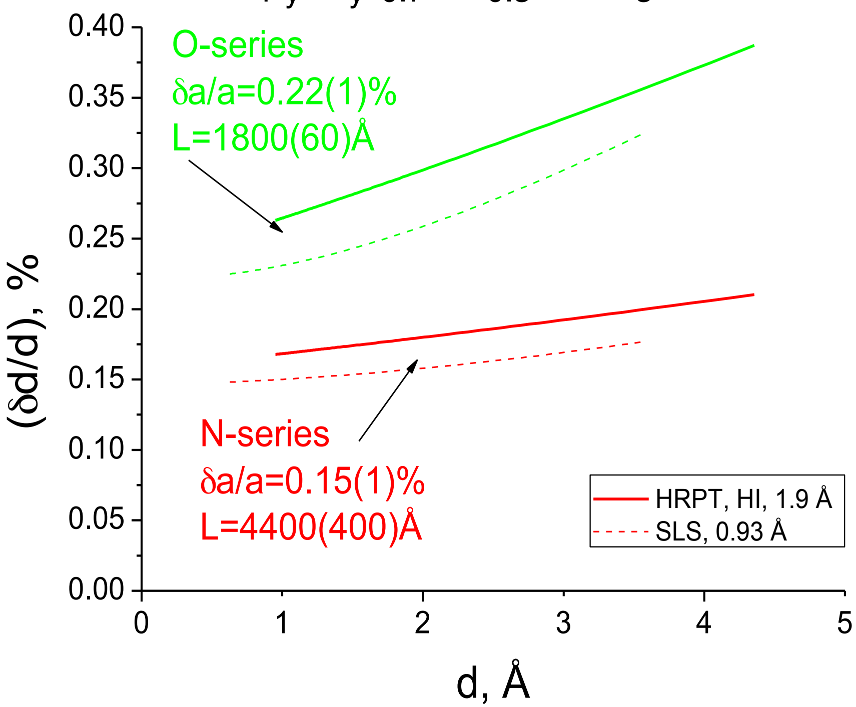

Instrumental resolution functions

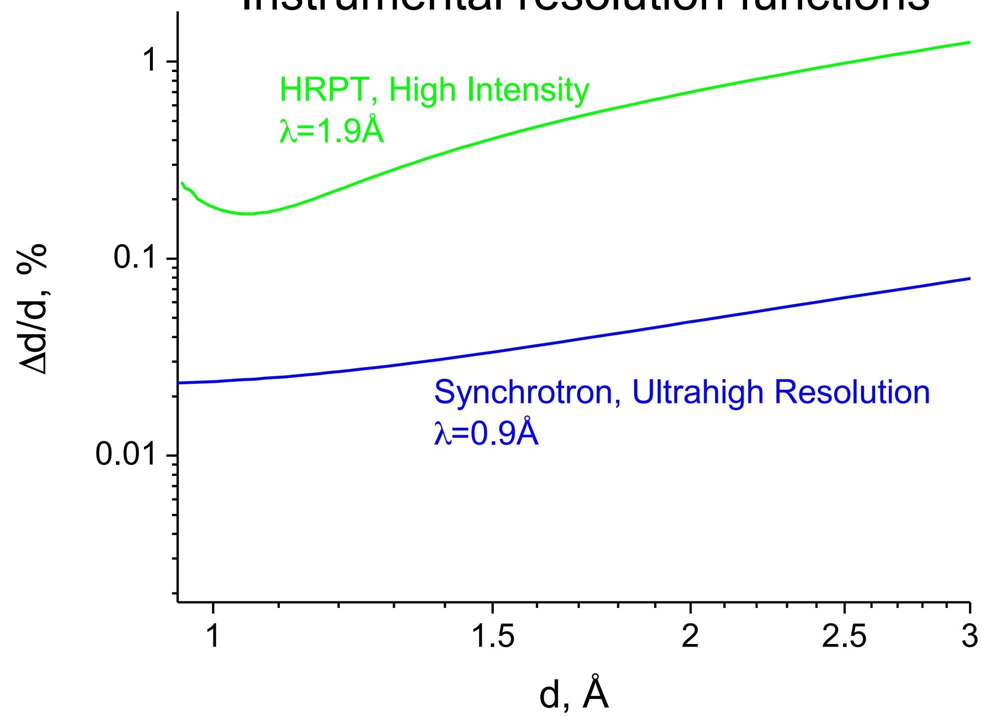

$$I_{\exp}(2\theta) = \int_{-\infty}^{\infty} PV_{sample}(2\theta - \xi) PV_{instrument}(\xi) d\xi$$

Lorenzian ⊗ Gaussian

Thermal cycling through T_C

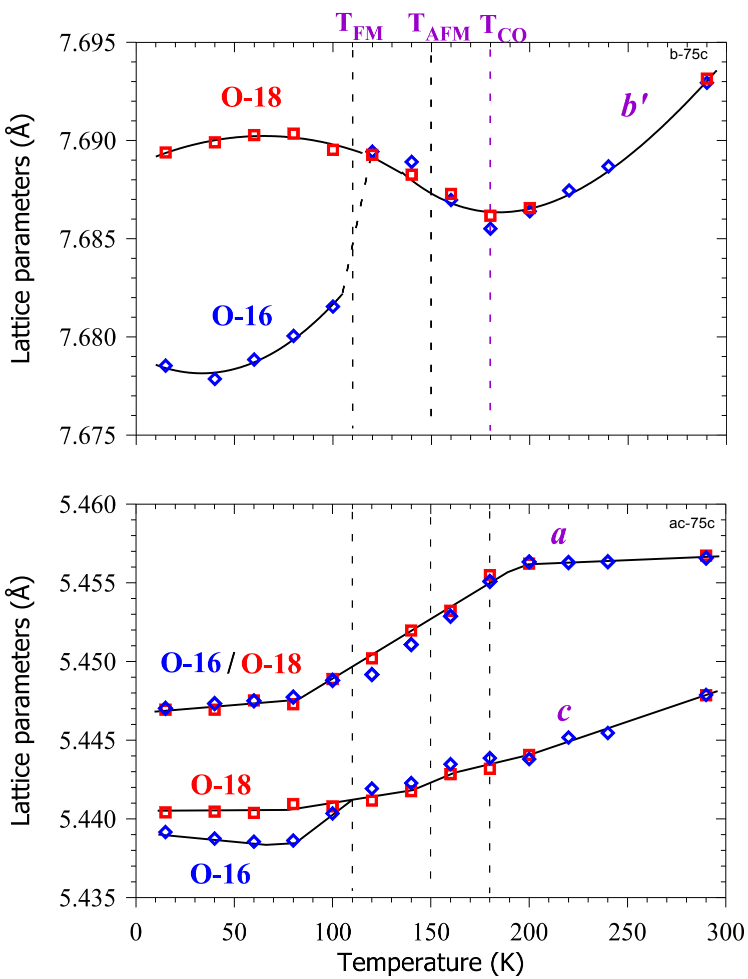

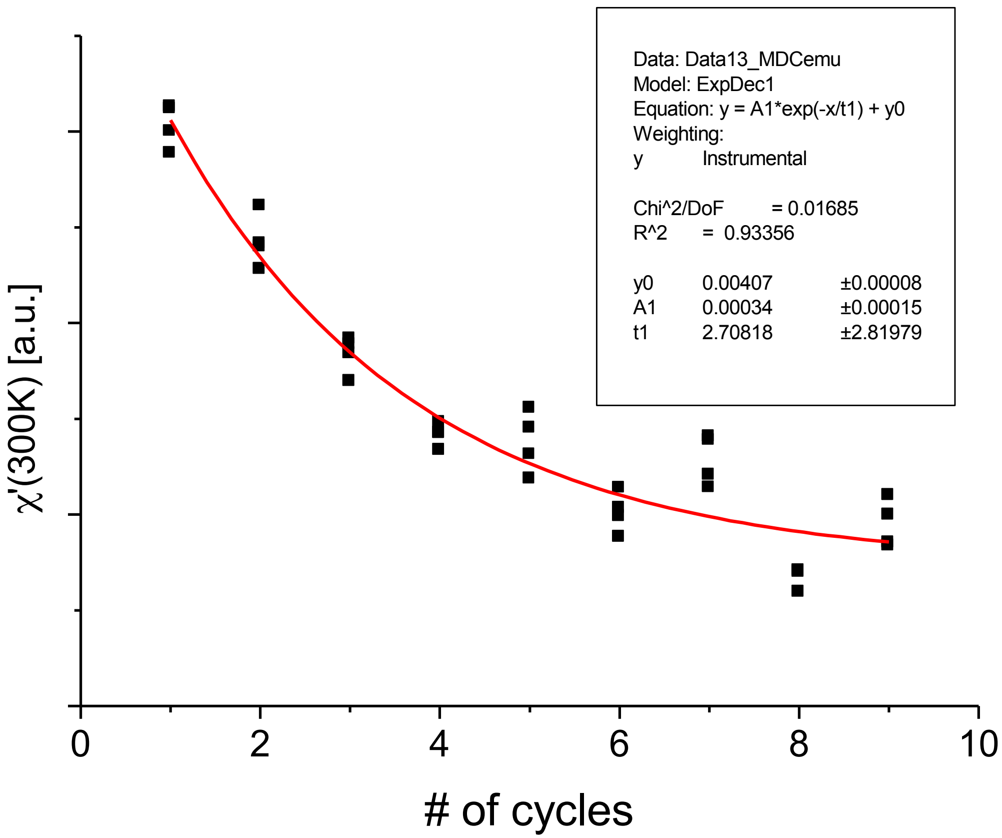

y=0.75

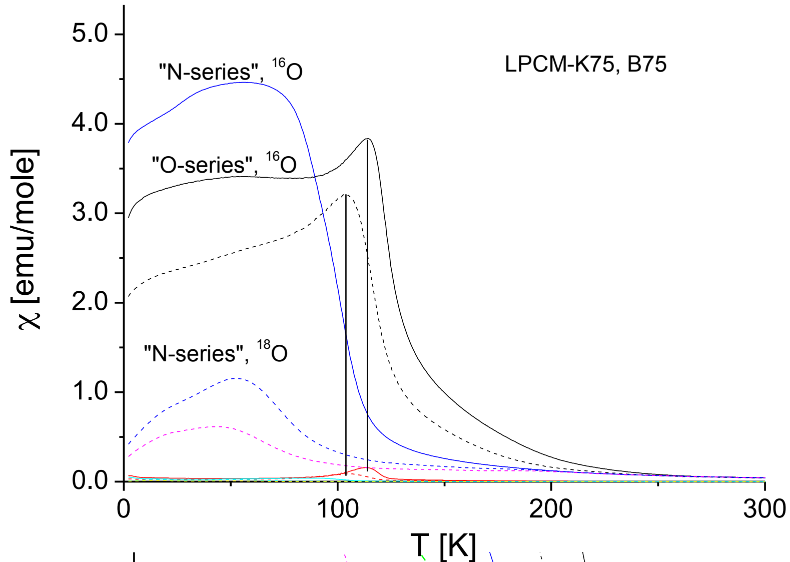

LPCM-K75, B75
"N-series", 16O
"O-series", 16O
"N-series", 18O
χ [emu/mole]
T [K]
5.0
4.0
3.0
2.0
1.0
0.0
0
100
200
300

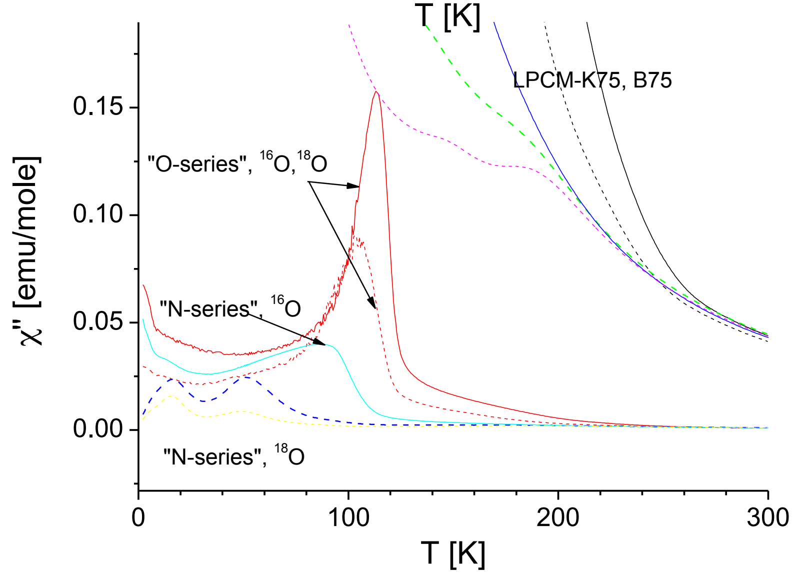

LPCM-K75, B75
"O-series", 16O,18O
"N-series", 16O
"N-series", 18O
χ'' [emu/mole]
T [K]
0.15
0.10
0.05
0.00
0
100
200
300

DMC pattern

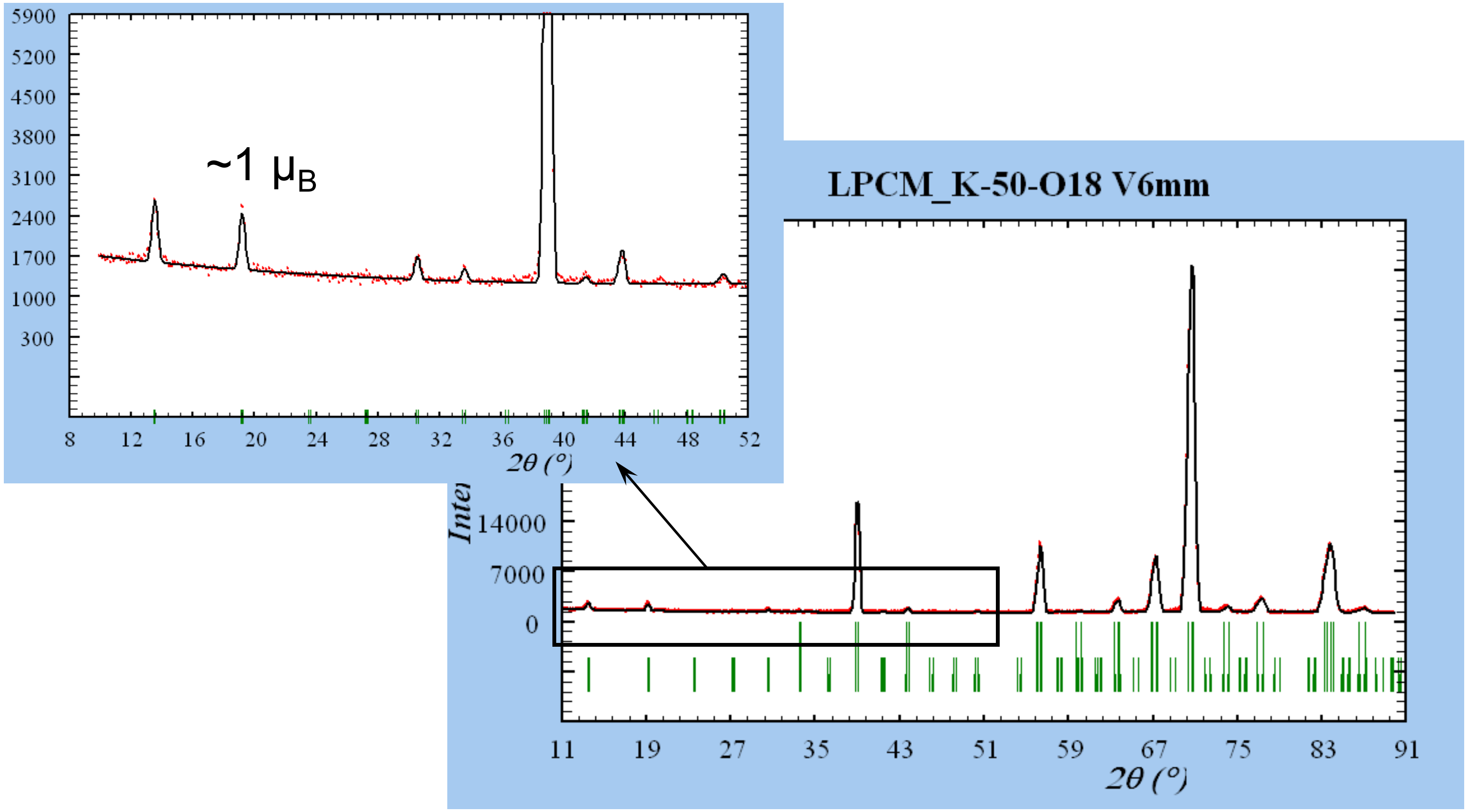

5900
5200
4500
3800
3100
2400
1700
1000
300
~1 μB
8 12 16 20 24 28 32 36 40 44 48 52
2θ (°)
LPCM_K-50-O18 V6mm
Inte
14000
7000
0
11 19 27 35 43 51 59 67 75 83 91
2θ (°)